From local to global relativity

Tuomo Suntola, www.sci.fi/~suntola

Newtonian physics is local by its nature. No local frame is in a special position in space. There are no overall limits to space or to physical quantities. Newtonian space is Euclidean until infinity, and velocities in space grow linearly as long as there is constant force acting on an object. Finiteness of physical quantities was observed for about 100 years ago – first as finiteness of velocities.

The theory of relativity introduces a mathematical structure for the description of the finiteness of velocities by modifying the coordinate quantities, time and distance for making the velocity of light appear as the maximum velocity in space and an invariant for the observer. Like in Newtonian physics, no local frame, or inertial observer, is in a special position in space. Friedman-Lemaître-Robertson-Walker (FLRW) metrics derived from the general theory of relativity predicts finiteness of space if a critical mass density in space is reached or exceeded.

In the Dynamic Universe approach space is described as the three-dimensional surface of a four-dimensional sphere. Finiteness of physical quantities in DU space comes from the finiteness of total energy in space — finiteness of velocities is a consequence of the zero-energy balance, which does not allow velocities higher than the velocity of space in the fourth dimension. The velocity of space in the fourth dimension is determined by the zero-energy balance of motion and gravitation of whole space and it serves as the reference for all velocities in space. Relativity in DU space means relativity of local to the whole — relativity is a measure of locally available share of the primary rest energy, the rest energy of the object in hypothetical homogeneous space. Atomic clocks in fast motion or in high gravitational field do not lose time because of slower flow of time but because part of their energy is bound into interactions in space. There is no space-time linkage in the Dynamic Universe; time is universal and the fourth dimension is metric by its nature. Local state of rest in DU space is the zero-momentum state in a local energy frame which is linked to hypothetical homogeneous space via a chain of nested energy frames.

Predictions for local phenomena in DU space are essentially the same as the corresponding predictions given by special and general theories of relativity. At extremes, at cosmological distances and in the vicinity of local singularities differences in the predictions become meaningful. Reasons for the differences can be traced back to the differences in the basic assumptions and in the structures of the two approaches.

1. Introduction

In its basic approach modern physics relies on Galilean and Newtonian tradition of connecting observer, observation and a mathematical description of the observation. Orientation to observations required the definition of observer's position and the state of rest. Newton's great breakthrough was the equation of motion, which linked acceleration to the mass of the accelerated object and thus defined the concept of force. The linkage of force to acceleration allowed the definition of gravitation as a force resulting in the acceleration of a falling object which allowed a physical interpretation of Kepler's laws of the motion of celestial bodies.

Newtonian physics is local by its nature. No local frame is in a special position in space. There are no overall limits to space or to physical quantities. Newtonian space is Euclidean until infinity, time is absolute without start or end, and velocities grow linearly as long as there is a constant force acting on an object. Velocities in Newtonian space summed up linearly without limitations.

The success of Newtonian physics led to a well-ordered mechanistic picture of physical reality. The nice Newtonian picture dominated until observations on the velocity of light in late 19th century when it turned out that the observer's velocity did not add the velocity of light which looked like an upper limit to all velocities.

In the theory of relativity the finiteness of velocities was solved by defining the coordinate quantities, time and distance, as functions of velocity and gravitational state so that the velocity of light appears as an invariant and the maximum velocity obtainable in space. In the framework of relativity theory, clocks in a high gravitational field and in fast motion conserve the local *proper time* but lose coordinate time related to time measured by a clock at rest in a zero gravitational field.

Like in Newtonian space, gravitation and motion in relativistic space are linked by *equivalence principle* equalizing inertial acceleration and gravitational acceleration. General appearance of relativistic space is derived assuming uniform distribution of mass at cosmological distances. Due to the local nature of the relativity theory, relativistic space conserves the gravitational energy and dimensions of local gravitational systems. The expansion of relativistic space occurs as “Hubble flow” in empty space between the local systems – probably speeded up by dark energy with gravitational push.

The need for relativity theory came from the observed finiteness of velocities and the unique property of the velocity of light as being insensitive to the velocity of the observer. The solution of modifying time and distance limit velocities in the spirit of relativity principle, but it does not account for the physical basis of such limitation. In specific areas of physics like in thermodynamics and quantum mechanics the system studied is specified by boundary conditions, the total energy of the system and a possible energy exchange from and to the system. Energy has been generally accepted as a primary conservable in closed systems.

Is there a way of studying whole space as a closed energy system and derive interactions and local limitations from the conservation of total energy in space?

In his lectures on gravitation in early 1960’s Richard Feynman [1] stated:

“If now we compare this number (total gravitational energy $M_\Sigma^2 G/R$) to the total rest energy of the universe, $M_\Sigma c^2$, lo and behold, we get the amazing result that $GM_\Sigma^2/R = M_\Sigma c^2$, so that the total energy of the universe is zero. — It is exciting to think that it costs nothing to create a new particle, since we can create it at the center of the universe where it will have a negative gravitational energy equal to $M_\Sigma c^2$. — Why this should be so is one of the great mysteries—and therefore one of the important questions of physics. After all, what would be the use of studying physics if the mysteries were not the most important things to investigate”.

and further [2]

“...One intriguing suggestion is that the universe has a structure analogous to that of a spherical surface. If we move in any direction on such a surface, we never meet a boundary or end, yet the surface is bounded and finite. It might be that our three-dimensional space is such a thing, a tridimensional surface of a four sphere. The arrangement and distribution of galaxies in the world that we see would then be something analogous to a distribution of spots on a spherical ball.”

Once we adopt the idea of the fourth dimension with metric nature, Feynman’s findings open up the possibility of a dynamic balance of space: the rest energy of matter is the energy of motion mass in space possesses due to the motion of space in the direction of the radius of the 4-sphere. Such a motion is driven by the shrinkage force resulting from the gravitation of mass in the structure. Like in a spherical pendulum in the fourth dimension, contraction building up the motion towards the center is followed by expansion releasing the energy of motion gained in the contraction.

The Dynamic Universe approach [3–9] is just a detailed analysis of combining Feynman’s “great mystery” of zero-energy space to the “intriguing suggestion of spherically closed space” by the dynamics of a four-sphere. The Dynamic Universe is a holistic model of physical reality starting from whole space as a spherically closed zero-energy system of motion and gravitation. Instead of extrapolating the cosmological appearance of space from locally defined field equations, locally observed phenomena are derived from the conservation of the zero-energy balance of motion and gravitation in whole space. The energy structure of space is described in terms of nested energy frames starting from hypothetical homogeneous space as the universal frame of reference and proceeding down to local frames in space. Time is decoupled from space – the fourth dimension has a geometrical meaning as the radius of the sphere closing the three-dimensional space.

In the Dynamic Universe, finiteness comes from the finiteness of the total energy in space — finiteness of velocities in space is a consequence of the zero-energy balance, which does not allow velocities higher than the velocity of space in the fourth dimension. The velocity of space in the fourth dimension is determined by the zero-energy balance of motion and gravitation of whole space and it serves as the reference for all velocities in space.

The total energy is conserved in all interactions in space. Motion and gravitation in space reduce the energy available for internal processes within an object. *Atomic clocks in fast motion or in high gravitational field in DU space do not lose time because of slower flow of time but because they use part of their total energy for kinetic energy and local gravitation in space.*

Relativity in Dynamic Universe does not need relativity principle, equivalence principle, Lorentz transformation, or postulation of the velocity of light. By equating the integrated gravitational energy in the spherical structure with the energy of motion created by momentum in the direction of the 4-radius we enter into zero-energy space with motion and gravitation in balance. Total energy of gravitation in spherically closed space is conserved in mass center buildup via local tilting of space which converts part of the gravitational interaction in the fourth dimension to gravitational interaction in a space direction and part of the velocity of space into velocity of free fall towards the local mass center created.

Relativity in Dynamic Universe means relativity of local to whole. Local energy is related to the total energy in space. As consequences, local velocities become related to the velocity of space in the fourth dimension and local gravitation becomes related to the total gravitational energy in space. Expansion of space occurs in a zero-energy balance of motion and gravitation. Local gravitational systems expand in direct proportion to the expansion of whole space.

The Dynamic Universe model allows a unified expression of energies and shows mass as wavelike substance for the expression of energies both in localized mass objects, in electromagnetic radiation, and Coulomb systems. The late 1800's great mystery of the invariance of the velocity of light in moving frames disappears as soon as we observe the momentum of radiation, not only the velocity. The momentum of radiation caught to a moving frame is changed due to the Doppler shift of frequency, not due to a change in velocity as observed in the case of catching mass objects to a moving frame. Equal Doppler change of wavelength and cycle time in detected radiation conserves the phase velocity but at a changed momentum.

2. Global approach to finiteness and relativity

2.1 Space as spherically closed energy structure

In the Dynamic Universe model a global approach to finiteness relies on the description of space as a closed energy system with potential energy and the energy of motion in balance. The structure closing the three dimensional space with minimum potential (gravitational) energy is the "surface" of a four dimensional sphere. Zero-energy balance in spherically closed space is obtained via interplay of the energies of motion and gravitation in the structure — in a contraction phase the energy of gravitation is converted into the energy of motion — in an expansion phase the energy of motion gained in the contraction is released back to the energy of gravitation, Fig. 2.1-1. In the contraction, space as a four-dimensional sphere releases volume and gains velocity. In the expansion, space releases velocity and gains volume.

Mathematically, the zero-energy dynamics of spherically closed space is expressed as

$$E_{rest(tot)} + E_{global(tot)} = M_\Sigma c_0^2 - \frac{GM''}{R_0} M_\Sigma = 0 \qquad (2.1{:}1)$$

where G is the gravitational constant, M_Σ is the total mass in space, $M'' = 0.776 \cdot M_\Sigma$ is the mass equivalence of the total mass (when concentrated into the center of the 4-sphere), R_0 is the radius of the 4-sphere, and c_0 is the velocity of contraction or expansion

$$c_0 = \pm\sqrt{\frac{GM''}{R_0}} = \pm\sqrt{\frac{0.776 \cdot G\rho 2\pi^2 R_0^3}{R_0}} = \pm 1.246 \cdot \pi R_0 \sqrt{G\rho} \qquad (2.1{:}2)$$

where ρ is the mass density in space.

Based on observations of the Hubble constant, space in its present state is in the expansion phase with radius R_0 equal to about 14 billion light years. By applying R_0 = 14 billion light years and by setting the mass density equal to $\rho = 5.0 \cdot 10^{-27}$ [kg/m^3], which is about half of the critical density ρ_0 in the standard cosmology model, velocity c_0 in (2.1:2) obtains the value $c_0 \approx c$ = 300 000 [km/s].

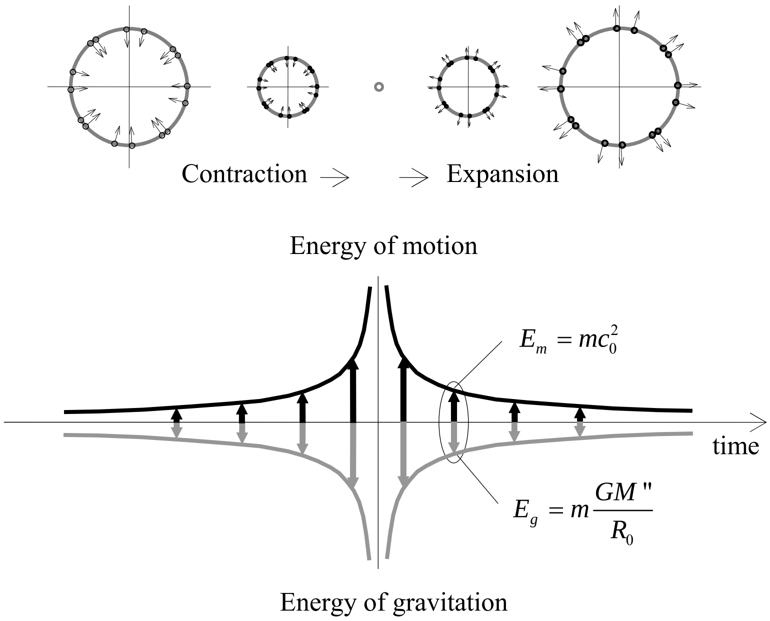

Figure 2.1-1. Energy buildup and release in spherical space. In the contraction phase, the velocity of motion increases due to the energy gained from release of gravitation. In the expansion phase, the velocity of motion gradually decreases, while the energy of motion gained in contraction is returned to gravity.

The contraction and expansion of spherically closed space is the primary energy buildup process creating the rest energy of matter as the complementary counterpart to the global gravitational energy.

For calculating the zero-energy balance in spherically closed space the inherent forms of the energies of gravitation and motion are defined as follows:

1) The inherent gravitational energy is defined *in homogeneous 3-dimensional space* as Newtonian gravitational energy

$$E_{g(0)} = -\rho mG\int_V \frac{dV(r)}{r} \tag{2.1:3}$$

where G is the gravitational constant, ρ is the density of mass, and r is the distance from mass m to volume differential dV. Total mass in homogeneous space is

$$M_\Sigma = \rho\int_V dV = \rho V \tag{2.1:4}$$

In spherically closed homogeneous 3-dimensional space the total mass is $M_\Sigma = \rho \cdot 2\pi^2 R_0^3$, where R_0 is the radius of space in the fourth dimension.

2) The inherent energy of motion is defined *in environment at rest* as the product of the velocity and momentum

$$E_{m(0)} = v|\mathbf{p}| = v|m\mathbf{v}| = mv^2 \tag{2.1:5}$$

The last form of the energy of motion in (2.1:5) has the form of the first formulation of kinetic energy, *vis viva*, “the living force” suggested by Gottfried Leibniz in late 1600’s [4].

The contraction – expansion process of space is assumed to take place in environment at rest, the underlying 4-dimensional universe. Accordingly, mass at rest in hypothetical homogeneous space has the inherent energy of motion

$$E_{m(0)} = c_0\,|\mathbf{p}_0| \tag{2.1:6}$$

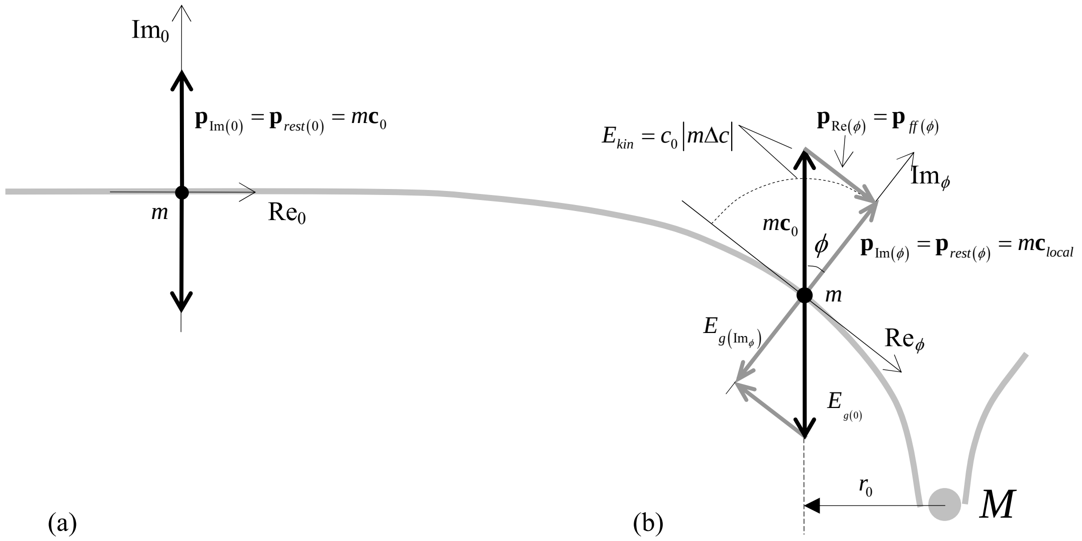

Figure 2.1-2. Conservation of the total energy of motion and gravitation in free fall towards a local mass center in space.

where c_0 is the velocity of space in the direction of the 4-radius, the fourth dimension. Velocity c_0 is conserved in all interactions in space. Locally, for the conservation of total gravitational energy, mass center buildup results in local tilting of space which converts momentum $\mathbf{p}_0$ into orthogonal components $\mathbf{p}_{\mathrm{Im}(\phi)}$ and $\mathbf{p}_{\mathrm{Re}(\phi)}$

$$E_{m(\phi),total} = c_0 |\mathbf{p}_0| = c_0 \left|\mathbf{p}_{\mathrm{Im}(\phi)} + \mathbf{p}_{\mathrm{Re}(\phi)}\right| = c_0 \left|\mathbf{p}_{rest(\phi)} + \mathbf{p}_{ff(\phi)}\right| \qquad (2.1:7)$$

which shows that the buildup of kinetic energy in free fall is achieved against reduction of the local rest energy

$$E_{kin(ff)} = c_0 \left|\mathbf{p}_{rest(0)} - \mathbf{p}_{rest(\phi)}\right| = c_0 |m\mathbf{c}_0 - m\mathbf{c}| = c_0 m \Delta c \qquad (2.1:8)$$

where the local velocity of light, which is equal to the velocity of space in the local fourth dimension is denoted as c ($c < c_0$), Fig. 2.1-2(b). The reduction of the global gravitational energy in tilted space is equal to the gravitational energy removed from the global spherical symmetry in homogeneous space

$$E_{g(\mathrm{Im}\phi)} = E_{g(\mathrm{Im}_0)} \left(1 - \delta\right) \qquad (2.1:9)$$

where δ is denoted as the local gravitational factor (=local gravitational energy/total gravitational energy)

$$\delta = \frac{GM}{r_0} \bigg/ \frac{GM''}{R_4} = \frac{GM}{c_0^2 r_0} = 1 - \cos\phi \qquad (2.1:10)$$

where r_0 is the distance of m from the local mass center M in the direction of non-tilted space. Tilting of local space in the vicinity of a local mass center means also reduction of the local velocity of light

$$c_{local} = c = c_0 \cos\phi = c_0 \left(1 - \delta\right) \qquad (2.1:11)$$

which together with the increased distance along the dent in space is observed as the Shapiro delay and the deflection of light passing a mass center in space. In real space mass center buildup occurs in several steps leading to a system of nested gravitational frames, Fig. 2.1.-3.

For each gravitational frame the surrounding space appears as apparent homogeneous space which serves as the closest reference to the global gravitational energy and the velocity of light in the local frame. Through the system of nested gravitational frames the local velocity of light is related to the velocity of light in hypothetical homogeneous space as

$$c_n = c = \prod_{i=1}^{n} c_0 \cos\phi \qquad (2.1:12)$$

The momentum of an object at rest in a gravitational state is the rest momentum in the direction of the local fourth dimension, the local imaginary direction.

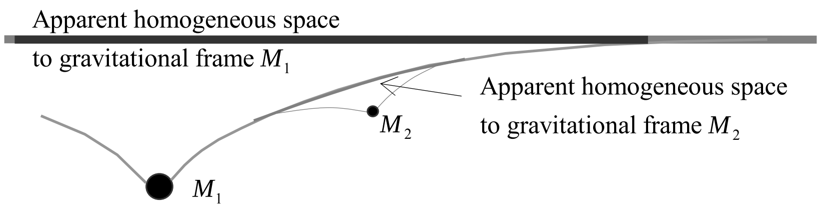

Figure 2.1-3. Space in the vicinity of a local frame, as it would be without the mass center, is referred to as apparent homogeneous space to the local gravitational frame. Accumulation of mass into mass centers to form local gravitational frames occurs in several steps. Starting from hypothetical homogeneous space, the "first-order" gravitational frames, like M_1 in the figure, have hypothetical homogeneous space as the apparent homogeneous space to the frame. In subsequent steps, smaller mass centers may be formed within the tilted space around in the "first order" frames. For those frames, like M_2 in the figure, space in the M_1 frame, as it would be without the mass center M_2, serves as the apparent homogeneous space to frame M_2.

Buildup of motion in a fixed gravitational state requires insert of mass via momentum in a space direction. The total energy of an object in motion comprises the components of the momentum in the imaginary direction and a space direction

$$E_{m(tot)} = c_0 \left|\mathbf{p}_{tot}\right| = c_0 \left|m\mathbf{c}_{\mathrm{Im}} + \mathbf{p}_{\mathrm{Re}}\right| = c_0 \sqrt{(mc)^2 + p^2} = c_0 (m + \Delta m) c \tag{2.1:13}$$

and the corresponding kinetic energy

$$E_{m(tot)} - E_{rest} = c_0 \Delta m \cdot c \tag{2.1:14}$$

A detailed analysis of the conservation of total energy of motion shows that the buildup of momentum in space reduces the rest momentum of the object in motion as

$$E_{rest(n)} = E_{rest(0)} \prod_{i=1}^{n} \sqrt{1-\beta_i^2} = c_0 m_0 c \prod_{i=1}^{n} \sqrt{1-\beta_i^2} = c_0 mc \tag{2.1:15}$$

where m is the mass, the substance for the expression of energy, available for the object in motion at velocities $\beta_i = v_i/c_i$ in the system of n nested frames, Fig. 2.1-4. Local velocity of space in the fourth dimension is not affected by the motion of an object. Accordingly, the square root term in (2.1:15) means a reduction of the rest mass of the moving object, which also means equal reduction in the global gravitational energy $E_{g,\mathrm{Im}(n)}$ of the moving object

$$m = m_0 \prod_{i=1}^{n} \sqrt{1-\beta_i^2} \tag{2.1:16}$$

Combining the effects of motion and gravitation on the rest energy of an object in the n:th frame results

$$E_{rest(n)} = E_{rest(0)} \prod_{i=1}^{n} (1-\delta_i) \sqrt{1-\beta_i^2} = c_0 mc \tag{2.1:17}$$

where c is the local velocity of light (2.1:12), which is a function of the gravitational state, and m is the locally available rest mass (2.1:16), which is a function of the motions of the object.

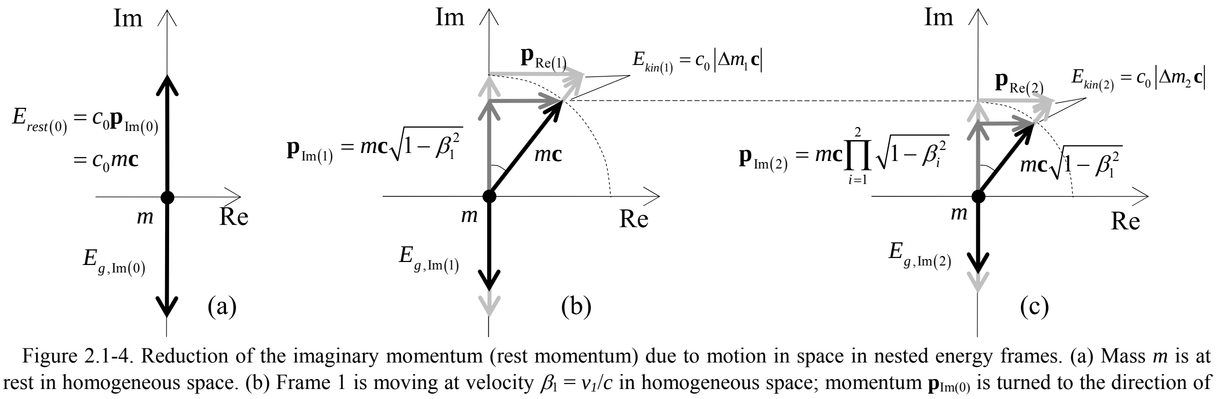

Figure 2.1-4. Reduction of the imaginary momentum (rest momentum) due to motion in space in nested energy frames. (a) Mass m is at rest in homogeneous space. (b) Frame 1 is moving at velocity $\beta_1 = v_1/c$ in homogeneous space; momentum $\mathbf{p}_{\mathrm{Im}(0)}$ is turned to the direction of total momentum with component $\mathbf{p}_{\mathrm{Re}(1)}$ in space (in the direction Re-axis). (c) Frame n is moving at velocity $\beta_n = v_n/c$ in frame 1; momentum $\mathbf{p}_{\mathrm{Im}(1)}$ is turned to the direction of total momentum with component $\mathbf{p}_{\mathrm{Re}(2)}$ in a space direction (in the direction Re-axis).

The energy of a quantum of radiation

In the DU framework the energy of a quantum of radiation appears as the unit energy carried by a cycle of radiation [6]

$$E_\lambda = c_0 \frac{h_0}{\lambda} c = c_0 m_\lambda c = c_0 \left|\mathbf{p}_\lambda\right| \qquad (2.1{:}18)$$

where $h_0 \equiv h/c$ is referred to as *intrinsic Planck constant* which is solved from Maxwell's equation, by observing that a point emitter in DU space which is moving at velocity c in the fourth dimension can be regarded as one-wavelength dipole in the fourth dimension. Such a solution shows also that the fine structure constant α is a purely numerical or geometrical factor without linkage to any physical constant. The quantity $h_0/\lambda \equiv m_\lambda$ [kg] in (2.1:18) is referred to as the mass equivalence of radiation.

Equally, Coulomb energy is expressed in form

$$E_C = \frac{e^2 \mu_0}{2\pi r} c_0 c = \alpha \frac{h_0}{2\pi r} c_0 c = c_0 m_C c \quad ; \quad \Delta E_C = c_0 c \cdot \Delta m_C \qquad (2.1{:}19)$$

where α is the fine structure constant and the quantity $\alpha \cdot h_0/2\pi r \equiv m_C$ is the mass equivalence of Coulomb energy.

Equations (2.1:17–19) give a unified expression of energies which is essential in a detailed energy inventory in the course of the expansion of space and in interactions within space. The zero-energy concept in the Dynamic Universe follows bookkeeper's logic — the accounts for the energy of motion and potential energy are kept in balance throughout the expansion and within any local frame in space.

The linkage between mass and wavelength or mass and wave number applies in both ways. The expression of mass in terms of the wavelength and wave number equivalences is

$$m = \frac{h_0}{\lambda_m} = \hbar_0 k_m \qquad (2.1{:}20)$$

which allows the expression of the total energy of motion or the DU equivalence of the "energy four-vector" in form

$$c_0^2 c^2 \; E_{m(total)}^2 = \left(c_0 mc\right)^2 + \left(c_0 p\right)^2 = c_0^2 c^2 \cdot \hbar_0^2 \left(k_{\mathrm{Im}(0)}^2 + k_{\mathrm{Re}(\beta)}^2\right) = c_0^2 c^2 \hbar_0^2 k_{\phi(\beta)}^2 \qquad (2.1{:}21)$$

or

$$k_{\mathrm{Im}(0)}^2 + k_{\mathrm{Re}(\beta)}^2 = k_{\phi(\beta)}^2 \qquad (2.1{:}22)$$

where

$$k_{\mathrm{Im}(0)} = \frac{m}{\hbar_0} \quad , \quad k_{\mathrm{Re}(\beta)} = \frac{\beta}{\sqrt{1-\beta^2}} \frac{m}{\hbar_0} \quad , \text{ and } \quad k_{\phi(\beta)} = \frac{1}{\sqrt{1-\beta^2}} \frac{m}{\hbar_0} \qquad (2.1{:}23)$$

Fig. 2.1-5.

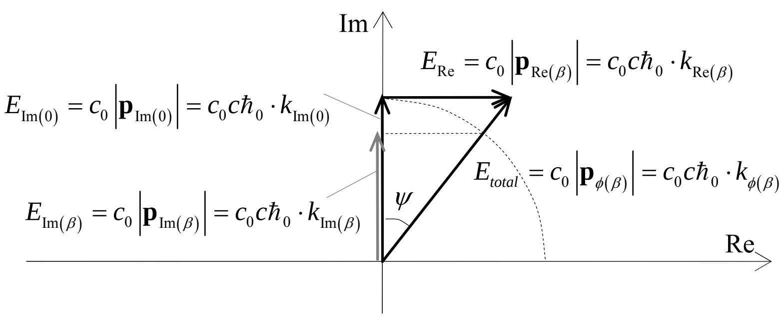

Figure 2.1-5. Complex plane presentation of the energy four-vector in terms of mass waves given in equation (2.1:22).

2.2 Relativity as the measure of locally available energy

Relativity in Dynamic Universe is observed as relativity of locally available rest energy to the rest energy the object has at rest in hypothetical homogeneous space. Relativity in Dynamic Universe is a direct consequence of the conservation of the total energy in interactions in space. It does not rely on relativity principle, spacetime, the equivalence principle, Lorentz covariance, or the invariance of the velocity of light — but just on the zero-energy balance of space.

The linkage of local and global is a characteristic feature of the Dynamic Universe. There are no independent objects in space — all local objects are linked to the rest of space.

The whole in the Dynamic Universe is not composed as the sum of elementary units — the multiplicity of elementary units is a result of diversification of the whole.

The rest energy that mass *m* possesses in the *n*:th energy frame is

$$E_{rest} = c_0 |\mathbf{p}| = c_0 mc = m_0 c_0^2 \prod_{i=1}^{n} (1-\delta_i)\sqrt{1-\beta_i^2} \tag{2.2:1}$$

where c_0 is the velocity of light in hypothetical homogeneous space, which is equal to the velocity of space in the direction of the 4-radius R_0. Momentum **p** in (2.2:1) is referred to as the rest momentum which appears in the local fourth dimension. The factors $\delta_i = GM_i/c^2$ and $\beta_i = v_i/c_i$ are the gravitational factor and the velocity factor relevant to the local frame, respectively. On the Earth, for example, the gravitational factors define the gravitational state of an object on the Earth, the gravitational state of the Earth in the solar frame, the gravitational state of the solar frame in the Milky Way frame, etc. The velocity factors related to an object on Earth comprise the rotational velocity of the Earth and the orbital velocities of each sub-frame in each one's parent frame.

An important message of equation (2.2:1) is that the effects of motion and gravitation on the rest energy of an object are different: motion at constant gravitational potential in a local frame releases part of the rest mass into the buildup of momentum in space – free fall in local gravitational field reduces the local rest momentum by reducing the velocity of space in the local fourth dimension via tilting of space.

Also, the buildup of kinetic energy (see equations 2.1:8 and 2.1:14) is different in inertial acceleration and in gravitational acceleration. Kinetic energy can be generally expressed as

$$E_{kin} = c_0 |\Delta \mathbf{p}| = c_0 \left(c|\Delta m| + m|\Delta c| \right) \tag{2.2:2}$$

where the first term shows the insert of mass in inertial acceleration and the second term shows the reduction of the velocity in space in the local fourth dimension. The first term is essentially equal to the kinetic energy in special relativity, the second term does not have direct counterpart in relativity theory which equalizes the effects of gravitational acceleration and inertial acceleration by the equivalence principle.

Equation (2.2:2) shows that the locally available rest energy is a function of the gravitational state, and the velocity of the object studied. Substituting (2.2:1) for the rest energy of electron in Balmer's equation the characteristic frequency related to an energy transition in atoms obtains the form

$$f_{local} = f_0 \prod_{i=1}^{n} (1-\delta_i)\sqrt{1-\beta_i^2} = f_{n-1}(1-\delta_n)\sqrt{1-\beta_n^2} \tag{2.2:3}$$

where frequency f_{n-1} is the characteristic frequency of the atom at rest in apparent homogeneous space of the local the local frame. The last form of equation (2.2:3) is essentially equal to the expression of coordinate time frequency on Earth, or Earth satellite clocks in the GR framework. The physical message of (2.2:3) is that *"the greater is the energy used for motions and gravitational interactions in space the less energy is left for running internal processes"*.

The Dynamic Universe links the energy of any localized object to the energy of whole space. Relativity in Dynamic Universe means relativity of local to the whole. At the cosmological scale an important consequence of the linkage between local space and whole space is that local gravitational systems grow in direct proportion to the expansion of space, thus, together with the spherical symmetry explaining the observed Euclidean appearance and surface brightnesses of galaxies in space. The magnitude versus redshift relation of a standard candle in the DU framework is in an accurate agreement with observations without assumptions of dark energy or any free parameter. Moreover, the zero-energy balance in the DU leads to stable orbits down to the critical radius in the vicinity of local singularities in space.

3. Comparison of local and global relativity

3.1 Definitions and basic quantities

Table 3.1-I gives a comparison of some fundamental quantities of relativity as described by special and general relativity and in the Dynamic Universe. The primary conservable in the DU framework is *mass as wavelike substance for the expression of energy*. Basic physical quantities are momentum and the energies of motion and gravitation, which are primarily defined in hypothetical homogeneous space. Force in the DU is a derived quantity as the negative of the gradient of energy. Electromagnetic energy is linked to mass via the mass equivalence of Coulomb energy and a cycle of radiation.

	Local relativity (SR&GR)	**Global relativity (DU)**
1) What is primarily finite in space?	Velocity	Total energy
2) Description of finiteness	$dt' = dt\sqrt{1-\beta^2}$ $dr' = dr\big/\sqrt{1-\beta^2}$	$E_{total} = M_\Sigma c_0^2 - \frac{GM''}{R_0} M_\Sigma = 0$
3) The velocity of light	$c \equiv$ constant by definition	The velocity of light is determined by the velocity of space in the fourth dimension, and the local tilting of space $c = c_0 \prod_{i=1}^{n} (1-\delta_i) = c_0 \prod_{i=1}^{n} \cos\phi_i$
3) Rest energy of mass m $(\beta = v/c)$	$E_{rest} = mc^2$	$E_{rest} = m_0 c_0^2 \prod_{i=1}^{n} (1-\delta_i)\sqrt{1-\beta_i^2}$
4) Kinetic energy $\left(\Delta m = m\left[1\big/\sqrt{1-\beta^2} - 1\right]\right)$ $\left(\Delta c = c_0\delta = \frac{GM}{r_0 c_0}\right)$	$E_{kin} = \Delta mc^2$	$E_{kin} = c_0\lvert\Delta\mathbf{p}\rvert = c_0\left(c\lvert\Delta m\rvert + m\lvert\Delta c\rvert\right)$
5) Planck constant	$h \equiv$ constant $\left[\text{kgm}^2/s\right]$	Solved from Maxwell's equations as the unit energy of a cycle of radiation $h_0 = 1.1049 \cdot 2\pi^3 e^2 \mu_0 \left(= \frac{h}{c}\right) \quad [\text{kg} \cdot \text{m}]$
6) Quantum of radiation	$E = h\nu$	$E_{\lambda(0)} = \frac{h_0}{\lambda} c_0 c = \hbar_0 k c_0 c = c_0 m_{\lambda(0)} c$ m_λ = mass equivalence of wave
7) Fine structure constant α	$\alpha \equiv \frac{e^2}{2h\varepsilon_0 c}$	$\alpha \equiv \frac{e^2\mu_0}{2h_0} = \frac{1}{1.1049 \cdot 2\pi^3}$

Table 3.1-I. Comparison of basic definitions and derived quantities for the rest energy, kinetic energy, and the velocities and cycle times in the vicinity of a mass center in the SR & GR framework and in the Dynamic Universe.

Differences between the two approaches result from the basic choice:

- In the framework of relativity theory finiteness in space is described *in terms of modified coordinate quantities*, which makes time and distance functions of velocity and the gravitational environment. The effect of gravitation relies on equivalence principle which links the acceleration in gravitational field to the inertial acceleration in the absence of gravitational field. Local rest energy is independent of the motion and gravitational environment of an objects.
- In the framework of Dynamic Universe finiteness in space is described as finiteness of total energy, which makes the locally available rest energy a function of energy reserved by motion and gravitation in space – via the velocity and gravitational potential of the local frame in its parent frames. Time and distance are universal in the DU.

In the SR&GR framework the velocity of light is constant by definition and the buildup of kinetic energy is described in terms of increase of effective mass – equally in the case of inertial acceleration in the absence of gravitational field and the case of free fall in gravitational field.

In the DU framework the buildup of kinetic energy is different in the case of acceleration via mass insert at constant gravitational potential and in acceleration via free fall in gravitational field. The physical meaning of the mass insert is demonstrated by the concept of mass equivalence, e.g. acceleration of a charged mass object in Coulomb field releases Coulomb energy in terms of a reduction of the mass equivalence as shown in equation (2.1:19). In the case of free fall in local gravitational field the buildup of kinetic energy occurs via tilting of local space against reduction of the local rest energy via a reduction of the velocity of space in the local fourth dimension, Table 3.1-I(4).

In the DU framework a point source of electromagnetic radiation can be studied as one-wavelength dipole in the fourth dimension. Solving the energy emitted by a dipole in an oscillation cycle results

$$E_{\lambda(0)} = \frac{P}{f} = \frac{N^2 e^2 z_0^2 \mu_0 16\pi^4 f^4}{12\pi c f} = N^2 \left(\frac{z_0}{\lambda}\right)^2 A \cdot 2\pi^3 e^2 \mu_0 c \cdot f \qquad (3.1:1)$$

For a point source with a singe unit charge ($z_0=\lambda$, $N=1$) the energy emitted in one cycle is the quantum

$$E_{\lambda(0)} = A_0 \cdot 2\pi^3 e^2 \mu_0 c_0 \cdot f = h_0 c_0 \cdot f = \hbar_0 k \cdot c c_0 = c_0 m_\lambda c \quad \left(= hf\right) \qquad (3.1:2)$$

where k is the wave number $k = 2\pi/\lambda$ and the quantity $\hbar_0 k$ has the dimension of mass [kg]. Factors A and A_0 are geometrical constants characteristic to the antenna. For an ordinary one wavelength dipole in space $A= 2/3$, for a point source as dipole in the fourth dimension $A_0 =1.1049$. Equation (3.1:2) breaks down the Planck constant into primary electrical constants; the unit charge (e), and the vacuum permeability (μ_0). In the *intrinsic Planck constant (h_0)* used in the DU framework the velocity of light (as a non-constant quantity) is removed. As a result the unit of the intrinsic Planck constant is [kg·m] instead of [kgm^2/s] like the traditional Planck constant, Table 3.1-I(5,6). *The removal of the velocity of light from the Planck constant links the concept of quantum to mass rather than to momentum.* The breakdown of the Planck constant into primary constants shows the fundamental nature of the fine structure constant as number independent of any physical constant, Table 3.1-I(7).

Localized mass object is described as a closed standing (mass)wave structure as illustrated with a one-dimensional resonator in Figure 3.1-1. The external momentum of a mass object moving in space at velocity β can be expressed as the sum of momentums of the Doppler shifted front wave and back wave

$$\mathbf{p}_{\mathrm{Re}(\beta)} = \frac{\hbar_0 k_0}{\sqrt{1-\beta^2}}\left[\tfrac{1}{2}(1+\beta) - \tfrac{1}{2}(1-\beta)\right]\mathbf{c} = \hbar_0 k_0 \frac{\beta}{\sqrt{1-\beta^2}}\mathbf{c} = \hbar_0 k_{DeBroglie}\mathbf{c} \qquad (3.1:3)$$

or a wave front with wave number k_β propagating in parallel with the object at velocity $\mathbf{v} = \beta\mathbf{c}$

$$\mathbf{p}_{\mathrm{Re}(\beta)} = \hbar_0 \frac{k_0}{\sqrt{1-\beta^2}}\beta\mathbf{c} = \hbar_0 k_\beta \mathbf{v} \qquad (3.1:4)$$

where the wave number k_β is equal to the wave number of the effective mass (relativistic mass), Fig. 3.1-1

$$k_\beta = \frac{k_0}{\sqrt{1-\beta^2}} = \frac{m_{eff}}{\hbar_0} \qquad (3.1:5)$$

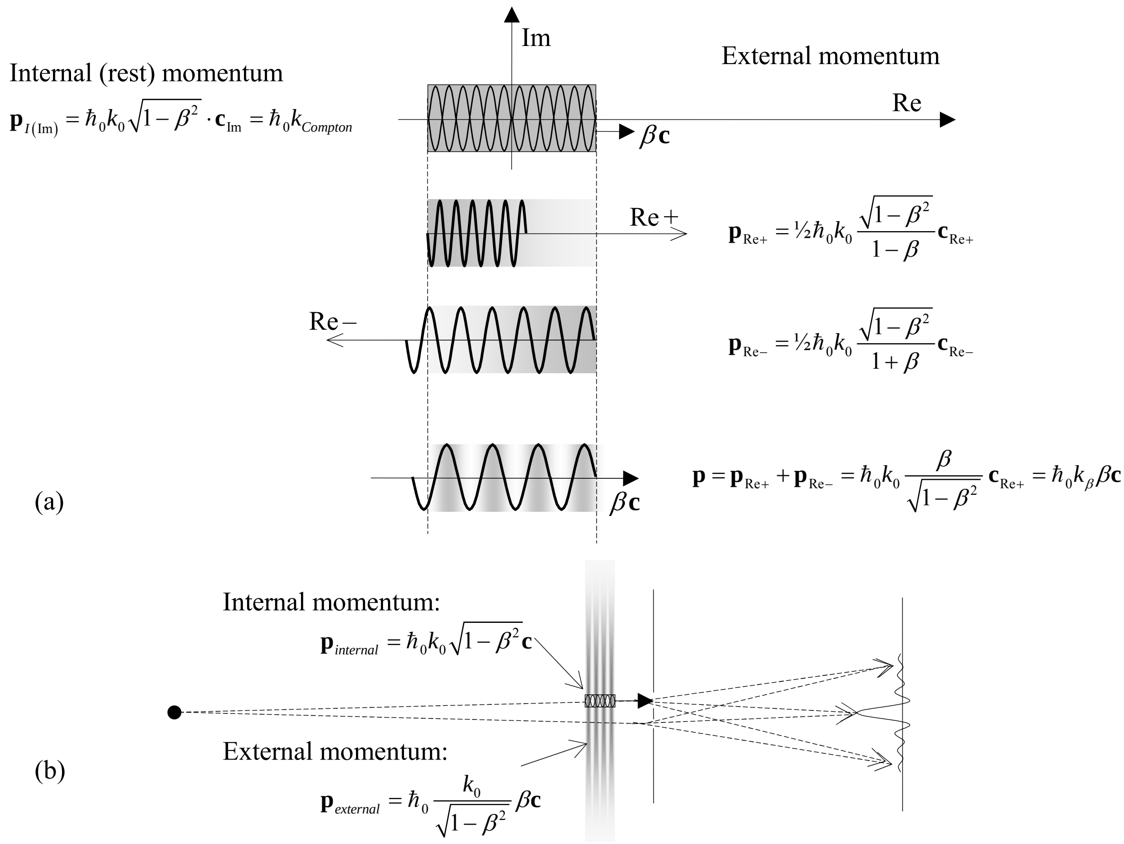

Figure 3.1-1(a). Mass object as one-dimensional standing wave structure (drawn in the direction of the real axis) moving at velocity β. The momentum in space is the external momentum as the sum of the Doppler shifted front and back waves, which is observed as the momentum of a wave front propagating in the parent frame in parallel with the propagating mass object. (b) In the double slit experiment the deflection of the propagation path is determined by the external momentum which is subject to interference pattern of the divided wave fronts from the slit.

A physical interpretation of equation (3.1:4) is that a mass object moving in space is associated with a parallel wave front carrying the external momentum the object in the parent frame.

This is exceedingly important as a physical explanation to the double-slit experiment. An energy object carries the rest energy as a standing wave in a localized energy structure. The external momentum appears as wave front k_β propagating at velocity β in parallel with the localized object. The wave front is subject to buildup of interference patterns on the screen when passing through the slits. The deflection angle of a singe object is determined by the phase difference between the wave fronts from the slits, Fig. 3.1-1(b).

3.2 Gravitation in Schwarzschild space and in DU space

Table 3.2-I summarizes some predictions related to celestial mechanics in Schwarzschild space which is the GR counterpart of the DU space in the vicinity of a local mass center in space.

At low gravitational field, far from the mass center the velocities of free fall as well as the orbital velocities in Schwarzschild space and DU space are essentially same as the corresponding Newtonian velocities. Close to critical radius, however, differences become meaningful.

In Schwarzschild space the critical radius is

$$r_{c(Schwd)} = \frac{2GM}{c^2} \tag{3.2:1}$$

which is the radius where Newtonian free fall from infinity achieves the velocity of light. Critical radius in DU space is

$$r_{c(DU)} = \frac{GM}{c_0 c_{0\delta}} \approx \frac{GM}{c^2} \tag{3.2:2}$$

	Local relativity (SR&GR)	Global relativity (DU)
1) Velocity of free fall $\left(\delta = GM/rc^2\right)$	$\beta_{ff} = \sqrt{2\delta}\left(1-2\delta\right)$ (coordinate velocity)	$\beta_{ff} = \sqrt{1/\left(1-\delta\right)^2 - 1}$
2) Orbital velocity at circular orbits	$\beta_{orb} = \dfrac{1-2\delta}{\sqrt{1/\delta - 3}}$ (coordinate velocity)	$\beta_{orb} = \sqrt{\delta\left(1-\delta\right)^3}$
3) Orbital period in Schwarzschild space (coordinate period) and in DU space	$P = \dfrac{2\pi r}{c}\sqrt{\dfrac{2}{\delta}}$ $\left(= P_{Newton}\right)$ $r > 3\cdot r_{c(Schwd)}$	$P = \dfrac{2\pi r_c}{c_{0\delta}}\left[\delta\left(1-\delta\right)\right]^{-3/2}$
4) Perihelion advance for a full revolution	$\Delta\psi\left(2\pi\right) = \dfrac{6\pi G\left(M+m\right)}{c^2 a\left(1-e^2\right)}$	$\Delta\psi\left(2\pi\right) = \dfrac{6\pi G\left(M+m\right)}{c^2 a\left(1-e^2\right)}$

Table 3.2-I. Predictions related to celestial mechanics in Schwarzschild space [11] and in DU space.

which is half of the critical radius in Schwarzschild space. The two different velocities c_0 and $c_{0\delta}$ in (3.2:2) are the velocity of hypothetical homogeneous space the velocity of apparent homogeneous space in the fourth dimension.

In Schwarzschild space the predicted orbital velocity at circular orbit exceeds the velocity of free fall when r is smaller than 3 times the Schwarzschild critical radius, which makes stable orbits impossible. In DU space orbital velocity decreases smoothly towards zero at $r = r_{c(DU)}$, which means that there are stable slow orbits between $0 < r < 4\cdot r_{c(DU)}$, Fig. 3.2-1(a,b).

The importance of the slow orbits near the critical radius is that they maintain the mass of the black hole.

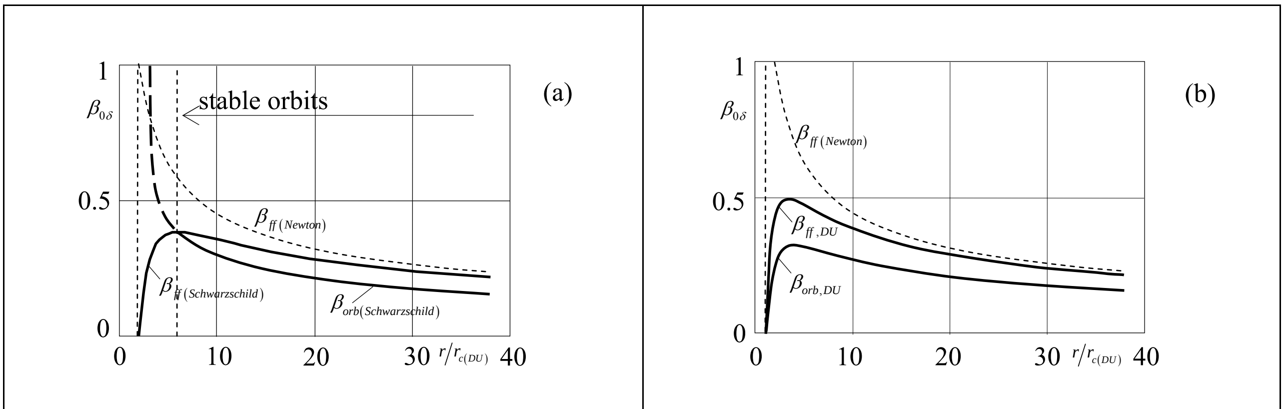

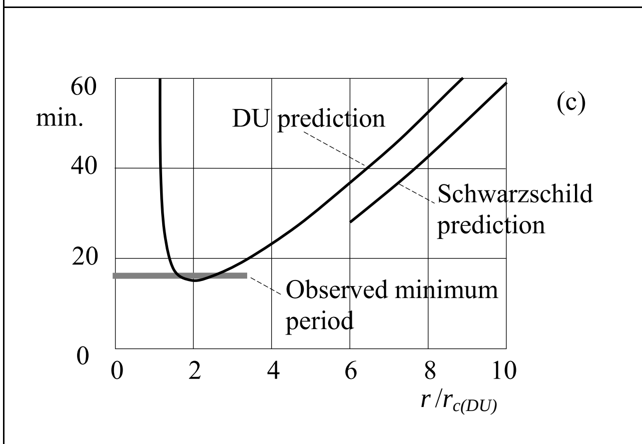

Figure 3.2-1. a) The velocity of free fall and the orbital velocity at circular orbits in Schwarzschild space,

b) The velocity of free fall and the orbital velocity at circular orbits in DU space. The velocity of free fall in Newtonian space is given as a reference. Slow orbits between $0 < r < 4\cdot r_{c(DU)}$ in DU space maintain the mass of the black hole.

c) The predictions by Schwarzschild and DU for period (in minutes) at circular orbits around Sgr A* in the center of Milky Way. The shortest observed period is 16.8 ± 2 min [8] which is very close to the minimum period 14.8 minutes predicted by DU. Minimum period predicted in Schwarzschild space is about 28 minutes, which occurs at $r = 3\cdot r_{c(Schwd)} = 6\cdot r_{c(DU)}$.

The prediction for the orbital period at circular orbits in Schwarzschild space apply only for radii $r > 3{\cdot}r_{c(Schwd)}$. The black hole at the center of the Milky Way, compact radio source Sgr A*, has the estimated mass of about 3.6 times the solar mass which means $M_{black\ hole} \approx 7.2{\cdot}10^{36}$ kg, which gives a period of 28 minutes at the minimum stable radius $r = 3{\cdot}r_{c(Schwd)}$ in Schwarzschild space. The shortest observed period at Sgr A* is 16.8 ± 2 min [12] which is very close to the prediction of minimum period 14.8 min in DU space at $r = 2{\cdot}r_{c(DU)}$, Fig. 3.2-1(c).

Prediction for perihelion advance in elliptic orbits is essentially the same in Schwarzschild space and in DU space. In DU space the prediction can be derived in a closed mathematical form.

3.3 Clocks and electromagnetic radiation in GR and DU

In DU space the prediction for the characteristic emission and absorption frequency related to energy transitions in hydrogen like atoms is obtained by substituting equation (2.2:1) for rest energy into Balmer's equation resulting

$$f_{(n1,n2)} = \frac{\Delta E_{(n1,n2)}}{h_0 c} = f_{0(n1,n2)} \prod_{i=1}^{n} \left(1-\delta_i\right)\sqrt{1-\beta_i^2} \qquad (3.3:1)$$

where $f_{0(n1,n2)}$ is the reference frequency for an atom at rest in hypothetical homogeneous space. Frequency $f_{0(n1,n2)}$ is subject to decrease in the course of the expansion of space

	Local relativity (SR&GR)	**Global relativity (DU)**
1) Flow of time (proper time) in Schwarzschild space and the frequency of a clock DU space	$d\tau = dt\sqrt{1-2\delta-\beta^2}$	$f = f_{0,0}\left(1-\delta\right)\sqrt{1-\beta^2}$
2) Gravitational red/blue shift. Frequency of electromagnetic radiation transmitted from higher to lower altitude (gravitation potential)	Frequency increases, velocity of light is conserved, wavelength decreases (= gravitational blueshift)	Frequency is conserved, the velocity of light decreases, wavelength decreases (=gravitational blueshift) (the observed frequency looks increased when compared to the frequency of a reference oscillator at receiver's gravitational state)
3) Shapiro delay (D_1,D_2 >> d)	$\Delta t_{D1,D2} = \frac{2GM}{c^3}\ln\left[\frac{4D_1D_2}{d^2}\right]$	$\Delta t_{D1,D2} = \frac{2GM}{c^3}\left\{\ln\left[\frac{4D_1D_2}{d^2}\right]-1\right\}$
4) Shapiro delay of radar signal (in radial direction to and from a mass center)	$\Delta t_{(A-B)} = \frac{2GM}{c^3}\ln\frac{r_B}{r_A}$	$\Delta t_{(A-B)} = \frac{2GM}{c^3}\ln\frac{r_B}{r_A}$
5) Bending of light path	$\phi = \frac{4GM}{c^2 d}$	$\phi = \frac{4GM}{c^2 d}$
6) Doppler effect	$f_{A(B)} = f_B\frac{\sqrt{1-\delta_A-\beta_A^2}\left(1-\beta_{B(\mathbf{r})}\right)}{\sqrt{1-\delta_B-\beta_B^2}\left(1-\beta_{A(\mathbf{r})}\right)}$	$f_{A(B)} = f_B\frac{\prod_{j=k+1}^{n}\left(1-\delta_{Bj}\right)\sqrt{1-\beta_{Bj}^2}\left(1-\beta_{jB(\mathbf{r})}\right)}{\prod_{i=k+1}^{m}\left(1-\delta_{Ai}\right)\sqrt{1-\beta_{Ai}^2}\left(1-\beta_{iA(\mathbf{r})}\right)}$

Table 3.3-I. summarizes some predictions related to the characteristic frequency of atomic oscillators (or proper time) and the propagation of electromagnetic radiation in space.

$$f_{0(n1,n2)} = Z^2\left[\frac{1}{n_1^2}-\frac{1}{n_2^2}\right]\frac{\alpha^2 m_{e(0)}}{2h_0}\left(\frac{2}{3}GM''\right)^{1/3} t^{-1/3} \qquad (3.3:2)$$

where t is the time since singularity. Characteristic frequencies are directly proportional to the velocity of light, both locally and in the course of the expansion of space which at present state of the expansion is about $dc_0/c_0 \approx 3.6\cdot10^{-11}$ /year.

The wavelength of radiation emitted is

$$\lambda_{(n1,n2)} = \frac{c}{f_{(n1,n2)}} = \frac{\lambda_{0(n1,n2)}}{\prod_{i=1}^{n}\sqrt{1-\beta_i^2}} \qquad (3.3:3)$$

which is independent of the velocity of light but subject to an increase with the motion of the emitter. The Bohr radius of atom is directly proportional to the wavelength emitted, which means that the atomic dimensions are independent of the expansion of space.

The proper time frequency in Schwarzschild space is

$$f_{\delta,\beta(GR)} = f_{0,0}\sqrt{1-2\delta-\beta^2} \approx f_{0,0}\left(1-\delta-\frac{1}{2}\beta^2-\frac{1}{8}\beta^4-\frac{1}{2}\delta\beta^2-\frac{1}{2}\delta^2\right) \qquad (3.3:4)$$

The corresponding prediction in DU space is the last form of equation (3.3:4)

$$f_{\delta,\beta(DU)} = f_{0,0}\left(1-\delta\right)\sqrt{1-\beta^2} \approx f_{0,0}\left(1-\delta-\frac{1}{2}\beta^2-\frac{1}{8}\beta^4+\frac{1}{2}\delta\beta^2\right) \qquad (3.3:5)$$

The difference between the GR and DU frequencies in equations (3.3:4) and (3.3:5) is

$$\Delta f_{\delta,\beta(DU-GR)} \approx \delta\beta^2 + ½\delta^2 \qquad (3.3:6)$$

In clocks on Earth and in Earth satellites the difference between the DU and Schwarzschild predictions is of the order $\Delta f/f \approx 10^{-18}$ which is too small a difference to be detected with present clocks. The difference, however, is essential at extreme conditions where δ and β approach unity, Fig. 3.3-1.

In DU space, atomic oscillators (or clocks) at different gravitation potentials have different frequency but the wavelength they emit is independent of the gravitational potential of the clock. This is because the frequency of the oscillator changes in direct proportion to the local velocity of light (the velocity of space in the local fourth dimension).

The frequency of electromagnetic radiation is conserved when transmitted from an emitter at one gravitational potential to a receiver at another gravitational potential. When compared to a reference oscillator at receiver's gravitational potential, the received frequency, however, is observed changed because the frequency of a reference oscillator at receiver's gravitational state is different from the frequency of the emitter at different gravitational potential, Fig. 3.3-2.

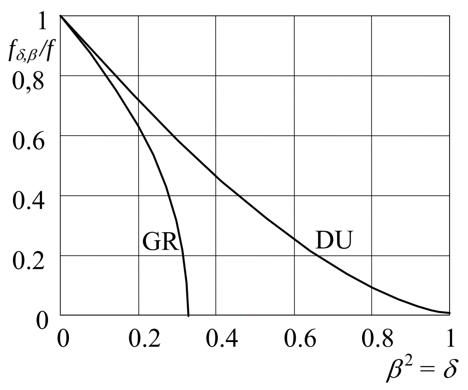

Figure 3.3-1. The difference in the DU and GR predictions of the frequency of atomic oscillators at extreme conditions when $\delta = \beta^2 \rightarrow 1$. Such condition may appear close to a black hole in space. The GR and DU predictions in the figure are based on equations (3.2:4) and (3.2:5), respectively.

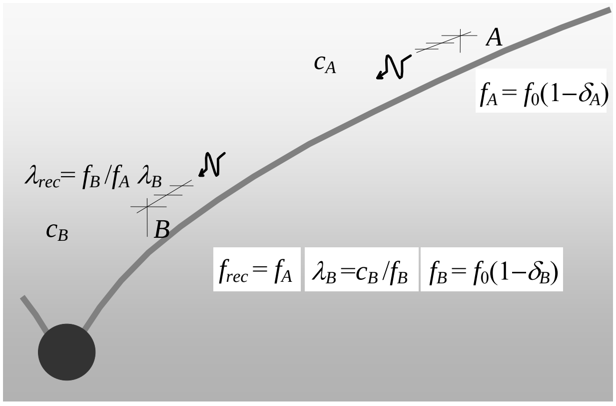

Figure 3.3-2. The velocity of light is lower close to a mass center, $c_B < c_A$, which results in a decrease of the wavelength of electromagnetic radiation transmitted from *A* to *B*. Accordingly, the signal received at *B* is blueshifted relative to the reference wavelength observed in radiation emitted by a similar object in the δ_B-state. The frequency of the radiation is unchanged during the transmission.

There is a small difference in the predictions of Shapiro delay in Schwarzschild space and in DU space. In DU space the velocity of light affect equally in the radial and tangential components of the light path but the lengthening of the path due to the tilting of space occurs only for the radial component of the path. In the Schwarzschild derivation both the effects of proper time and the lengthening of the path are calculated for both the tangential and radial component of the light path, Table 3.3-1(3). If this were not the case it meant different velocity of light in the radial and tangential directions in Schwarzschild space, Fig. 3.3-3. When the tangential component of light path is zero, i.e. the signal path has radial direction to and from a mass center, the difference between the predictions vanishes, Table 3.3-1(4).

In the Mariner 6 and 7 experiments [13] in 1970’s the signal delay was studied by comparing the delays at different passing distances *d* between the signal path and the Sun, i.e. the case of Table 3.3-I(3). In Mariner experiments, due to the lack of an absolute reference, the constant term in the DU prediction in Table 3.3-I(3) becomes ignored which means that the experiment is not able to distinguish the difference of the GR and DU predictions which in the Mariner case is 20 μs at any passing distance (in the 160 to 200 μs total delay).

Prediction for the bending of light in the vicinity of a mass center according to the GR and DU are equal, Table 3.3-I(5). It means that predictions for gravitational lensing in the two frameworks are equal.

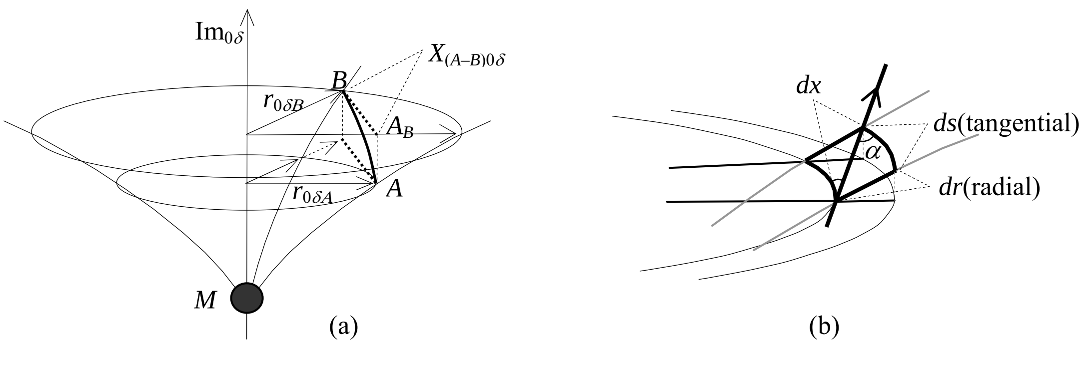

Figure 3.3-3. (a) Light path *AB* from location *A* to location *B* follows the shape of the dent in space as a geodesic line in the gravitational frame of mass center *M*. Point *A* is at flat space distance $r_{0\delta A}$ and point *B* is at flat space distance $r_{0\delta B}$ from mass center *M*. Point A_B is the flat space projection of point A on the flat space plane crossing point B. Line A_BB is the distance between A and *B* as it would be without the dent. The velocity of light in the dent is reduced in proportion to $1/r_{0\delta}$, i.e. the velocity of light at *A* is higher than the velocity of light at *B*. Distance AB_A is the projection of path *AB* on the flat space plane. (b) The difference in the predictions of Shapiro delay in Schwarzschild space and in DU space is due to a different effect of the local tilting of space on the tangential component of the light path. In DU space the velocity of light affect equally in the radial and tangential components of the light path but the lengthening of the path occurs only in for the radial component of the path. In the Schwarzschild derivation both the effects of proper time and the lengthening of the path are calculated for both the tangential and radial component of the light path. If this were not the case it meant different velocity of light in the radial and tangential directions in Schwarzschild space where *dt* instead of *c* (like in the DU) is a function of the gravitational state.

The Doppler effect of electromagnetic radiation in the GR framework is expressed in terms of local Schwarzschild space; in the DU prediction also the motions and gravitational state of the source and receiver in the parent frames are taken into account, Table 3.3-I(6). For source and receiver in the same gravitational frame the predictions are equal. The Doppler effect in Table 3.3-I(6) does not include the effect of the expansion of space which results in further frequency shift at cosmological distances.

The Doppler effect of electromagnetic radiation increases equally the frequency and the wave number of radiation observed in a frame moving in the direction of the radiation. For radiation sent at rest in a local frame and received by an observer moving in the direction of the radiation in the same gravitational state the observed angular frequency is (both according to GR and DU predictions)

$$\omega_{A(B)} = \frac{\omega_B}{\sqrt{1-\beta_B^2}}\left(1-\beta_{B(\mathbf{r})}\right) = \omega_A\left(1-\beta_{B(\mathbf{r})}\right) \qquad (3.2.4:4)$$

and the observed wave number $k = 2\pi/\lambda$

$$k_{A(B)} = \frac{k_B}{\sqrt{1-\beta_B^2}}\left(1-\beta_{B(\mathbf{r})}\right) = k_A\left(1-\beta_{B(\mathbf{r})}\right) \qquad (3.2.4:4)$$

which result in observed phase velocity

$$c_B = \frac{\omega_{A(B)}}{k_{A(B)}} = \frac{\omega_A}{k_A} = c_A \qquad (3.2.4:4)$$

i.e. the phase velocity observed in a frame moving with the observer, is equal to the phase velocity observed at rest in the parent frame, Table 3.3-II.

	Local relativity (Newtonian)	**Global relativity (DU)**
Observation of a mass object in a moving frame. v = velocity of the moving frame v_0 = velocity of the object in the parent frame	$\mathbf{p}_v = m\mathbf{v}_0\left(1-\frac{v}{v_0}\right) = \mathbf{p}_0\left(1-\frac{v}{v_0}\right)$ The change in momentum is observed as change in velocity	$\mathbf{p}_v = m\mathbf{v}_0\left(1-\frac{v}{v_0}\right) = \mathbf{p}_0\left(1-\frac{v}{v_0}\right)$ The change in momentum is observed as change in velocity
Observation of electromagnetic radiation in a moving frame c_0 = the velocity of light in the parent frame	$\mathbf{p}_v = \hbar\mathbf{k}_0\left(1-\frac{v}{c_0}\right) = \mathbf{p}_0\left(1-\frac{v}{c_0}\right)$ The change in momentum is observed as change in the wave number and frequency	$\mathbf{p}_v = \hbar_0 k_0\left(1-\frac{v}{c_0}\right)\mathbf{c}_0 = \mathbf{p}_0\left(1-\frac{v}{c_0}\right)$ The change in momentum is observed as change in the wave number and frequency
Phase velocity of radiation in moving frame	$c_v \equiv c_0$	$c_v = \frac{\omega_v}{k_v} = \frac{\omega_0\left(1-\frac{v}{c_0}\right)}{k_0\left(1-\frac{v}{c_0}\right)} = \frac{\omega_0}{k_0} = c_0$

Table 3.3-II. Transformation of the momentum of a mass object and the momentum of electromagnetic radiation observed in a frame moving at velocity v_{frame} in its parent frame. For simplicity, velocity v_{frame} is assumed small enough to allow ignoring the increase of the effective (relativistic) mass. The conclusion is that the (phase) velocity of light is observed unchanged without a specific definition of the constancy. The conclusion is the same also when the relativistic effects of mass increase are included.

The late 1800's great confusion of the conservation of the observed velocity of light in moving frames obtains a trivial solution once we study the moving frames as momentum frames instead of velocity frames:

The constancy of the observed (phase) velocity of light in moving frames is a consequence of the change of momentum via the Doppler shift of frequency (and mass equivalence) instead of change in the velocity as we observe the change of the momentum of mass objects.

Studying of the Michelson – Morley interferometer as a momentum frame moving in its parent frames guarantees a zero result.

3.4 Cosmological appearance of space derived from general relativity and the DU

At the cosmological scale, like the DU space, GR space is assumed to be isotropic and homogeneous; i.e., it looks the same from any point in space [14]. As a major difference to the Friedman-Lemaître-Robertson-Walker (FLRW) cosmology or ΛCDM cosmology (Lambda Cold Dark Matter cosmology), local gravitational systems in DU space are subject to expansion in direct proportion to the expansion of the 4-radius R_0. Accordingly, e.g., the radii of galaxies are not observed as standard rods but as expanding objects which makes the sizes of galaxies appear in Euclidean geometry to the observer.

As shown by an analysis of the Bohr radius, material objects built of atoms and molecules are not subject to expansion with space. Like the Bohr radius, the characteristic emission wavelengths of atomic objects are unchanged in the course of the expansion of space. When propagating in space, the wavelength of electromagnetic radiation is increased in direct proportion to the expansion. Accordingly, when detected after propagation in space, characteristic radiation is observed redshifted relative to the wavelength emitted by the corresponding transition in situ at the time of observation.

Major difference between FLRW space and DU space comes from the general cosmological appearance and the picture of reality. The expression of energy and the evolution of DU space is a continuous process from infinity in the past to infinity in the future under unchanged laws of nature. In the DU mass is not a form of energy but the substance for the expression of energy via excitation of motion against release of potential energy. Any local expression of energy in DU space is linked to the rest of space. Anti-energy for the rest energy of a mass object in space is the gravitational energy due to the rest of mass in space as indicated by zero-energy balance of the rest energy and the global gravitational energy. Relativity in DU space means relativity of local to the whole.

Table 3.4-I summarizes some general features of the FLRW space and the DU space. The difference between the local approach of the GR based FLRW space and the global approach of the DU space is well demonstrated by the scope of expansion: For conserving the gravitational energy in local systems expansion in FLRW space is assumed to occur between galaxies or galaxy groups only. In the DU local gravitation is a share of the total gravitational energy; dilution of the total gravitational energy in the expansion dilutes equally the gravitational energy of local systems, which is seen as the expansion of gravitationally bound local systems with the expansion of whole space.

Another important difference between the FLRW and DU models is the conservation of the energy of radiation propagating in space. In both models the wavelength of radiation is supposed to increase in direct proportion to the expansion of space. In the FLRW interpretation of the effect of redshift on the power density of radiation is based on the fundamental work of Hubble, Tolman, Humason, deSitter, and Robertson, in the 1930's [15–20]. After an active debate the conclusion was that the dilution of the power density of redshifted radiation comes from two factors: The reduced rate of quanta received, and the dilution of the energy of a quantum due to the reduced frequency as suggested by a direct interpretation of the Planck's equation. Combining these two effects the dilution of power density due to the expansion of FLRW space obtains the form

$$F_{z(FLRW)} = \frac{E_{0(z)}}{T_{0(z)}} = \frac{h \cdot f_{0(z)}}{T_{0(z)}} = \frac{h \cdot f_0 / (1+z)}{T_0 (1+z)} = \frac{E_0}{T_0} \Big/ (1+z)^2 = \frac{F_0}{(1+z)^2} \tag{3.4:1}$$

where $T_{0(z)}$ is the time required to receive a quantum of radiation (which in the DU framework is the cycle time). ***The dilution of the energy of a quantum means loss of total energy of radiation propagating in FLRW space.***

	FLRW space	DU space
The beginning	Big Bang, singularity of space about 13.7 billion years ago: start of time, turn-on of the laws of physics	The process of energy buildup and release via contraction and expansion works like pendulum from infinity in the past to infinity in the future. Time and the laws of physics are perpetual.
The future	The future development of the universe cannot be predicted.	The ongoing expansion continues to infinity in a zero-energy balance of motion and gravitation (see Fig. 2.1-1)
The shape of space	Undetermined space-time	Surface of 4-sphere
Expansion of space	Expansion occurs as Hubble flow between galaxies or galaxy groups only. Presently, the expansion is assumed to accelerate due to an increasing share of dark energy.	All gravitationally bound systems expand with the expansion of space. Expansion velocity decreases with time since singularity as $c_0 = \frac{dR_4}{dt} = \left(\frac{2}{3}GM''\right)^{1/3} t^{-1/3}$
Dilution of the power density of redshifted electromagnetic radiation	Wavelength of radiation is increased + the energy content of a quantum is diluted $F_z = F_0 / (1+z)^2$ Conservation of total energy is violated.	Wavelength of radiation is increased but the energy content of a quantum is conserved (= mass equivalence of a cycle of radiation is conserved) $F_z = F_0 / (1+z)$ Conservation of total energy is honored.
Antimatter	Disappeared at Big Bang	Antienergy of the rest energy of a mass object is the gravitational energy due to the rest of mass in space.
Dark matter	Existent, undefined	Unstructured matter (wavelike)
Dark energy	Existent, needed to match ΛCDM predictions to observations	Non-existent. DU predictions are consistent with observations without dark energy (or any other parameter).

Table 3.4-I. Comparison of the development and general appearance of FLRW space and DU space.

In the DU framework the conservation of the energy of radiation is seen as the conservation of the mass equivalence of radiation, i.e. the energy carried by a cycle of radiation

$$E_{0(z),\lambda} = m_\lambda c_0 c \tag{3.4:2}$$

where the mass equivalence m_λ of radiation is

$$m_\lambda = h_0 / \lambda_0 \tag{3.4:3}$$

and λ_0 is the wavelength emitted. An increase of the wavelength does not reduce the mass equivalence but dilutes it in volume and the cycle time when received. Conservation of the mass equivalence of radiation means that the lengthening of the wavelength dilutes density of mass carried by the wave and thus the power density observed but it does not lose mass

$$F_{z(DU)} = \frac{E_{0(z)}}{T_{0(z)}} = \frac{m_\lambda c_0 c}{T_{0(z)}(1+z)} = \frac{F_0}{1+z} \tag{3.4:4}$$

	FLRW cosmology	DU cosmology
1) Physical distance (co-moving distance)	$D_M = R_H \int_0^z \frac{1}{\sqrt{(1+z)^2(1+\Omega_m z) - z(2+z)\Omega_\Lambda}} dz$	$D = R_0 \ln(1+z)$
2) Angular diameter distance (referred to as optical distance in DU)	$D_A = R_H \frac{1}{1+z} \int_0^z \frac{1}{\sqrt{(1+z)^2(1+\Omega_m z) - z(2+z)\Omega_\Lambda}} dz$	$D = R_0 \frac{z}{1+z}$
3) Angular diameter of galaxies and quasars	$\theta = \frac{d_R(1+z)}{R_H} \Big/ \int_0^z \frac{1}{\sqrt{(1+z)^2(1+\Omega_m z) - z(2+z)\Omega_\Lambda}} dz$	$\theta = \frac{d_R}{D}(1+z) = \frac{d_R}{R_0}\frac{1}{z}$
4) Luminosity distance	$D_L = R_H (1+z) \int_0^z \frac{1}{\sqrt{(1+z)^2(1+\Omega_m z) - z(2+z)\Omega_\Lambda}} dz$	$D = R_0 \frac{z}{1+z}\sqrt{1+z}$
5) Magnitude for *K*-corrected observations	$m = M + 5\log\frac{R_H}{d_0}$ $+5\log\left[(1+z)\int_0^z \frac{1}{\sqrt{(1+z)^2(1+\Omega_m z) - z(2+z)\Omega_\Lambda}} dz\right]$	$m = M + 5\log\frac{R_0}{d_0}$ $+5\log\left[z^2(1+z)\right]$

Table 3.4-II. The factor (1+z) and the resulting Euclidean appearance in the DU prediction for angular diameter comes from the fact that the diameter of the galaxies and quasars increase in direct proportion to the expansion of space. Luminosity distance is the distance equivalence used to match the power density of redshifted radiation to the classical $F \sim 1/D^2$ formula. For making the DU prediction of magnitude comparable to the prediction of magnitude in FLRW cosmology [20] the effect of *K*-correction [22] is included. Detailed derivation of the DU predictions are given in Appendix A1.

When solved from Maxwell's equation [see equation (3.1:2)] the energy emitted into one cycle of radiation by a unit charge transition from a point source is

$$E = hf \quad \text{or} \quad E_{\lambda(0)} = 1.1049 \cdot 2\pi^3 e^2 \mu_0 c \cdot f \qquad (3.4:5)$$

The Planck equation describes the energy conversion at the emission of radiation as the insert of mass equivalence into a cycle of radiation. The Planck equation is not consistent for describing the conservation of mass equivalence carried by a cycle of radiation.

Table 3.4-II summarizes the predictions for three important distance definitions and the predictions for the angular size and magnitudes. The physical distance which means the momentary distance of objects, the angular diameter distance which is the distance of light path from the object to the observer in expanding space, and luminosity distance a distance equivalence of redshifted radiation for the classical definition of magnitude. The meaning of physical distance and the optical distance in DU-space are illustrated in Figure 3.4-1. A comparison of the predictions in Table 3.4-II(2) is given in Figure 3.4-2.

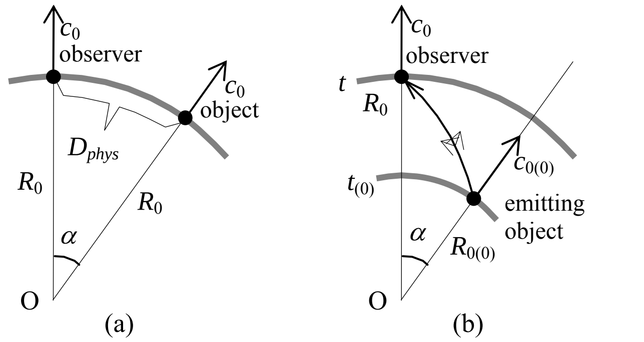

Figure 3.4-1. (a) The classical Hubble law corresponds to Euclidean space where the observed distance of the object is equal to the physical distance, the arc Dphys, at the time of the observation. (b) When the propagation time of light from the object is taken into account the observed distance is the optical distance which is the length of the integrated path over which light propagates in the tangential direction on the "surface" of the expanding 4-sphere. Because the velocity of light in space is equal to the expansion of space in the direction of R4, the optical distance is $D = R_0 - R_{0(0)}$, the lengthening of the 4-radius during the propagation time.

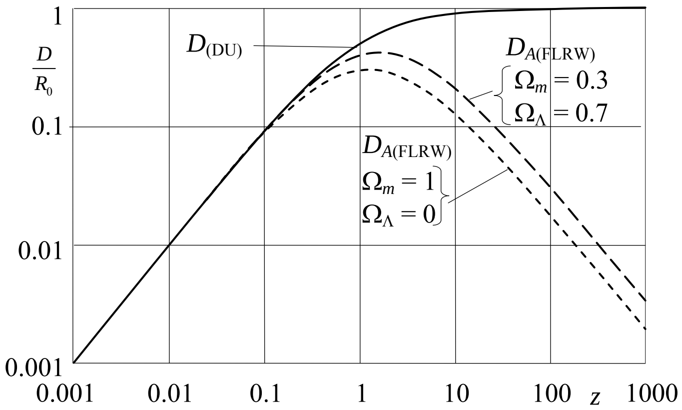

Figure 3.4-2. Optical distance of objects in DU space (solid line) and the angular diameter distance in FLRW space for $\Omega_m = 1$, $\Omega_\Lambda = 0$ and for $\Omega_m = 0.27$, $\Omega_\Lambda = 0.73$ corresponding to the Einstein-deSitter condition in FLRW space and the present estimates of mass and dark energy densities in ΛCDM corrected space, respectively (dashed lines).

In Figure 3.4-3 the DU prediction and the FLRW prediction for the angular diameter are compared to observations of the Largest Angular Size (LAS) of galaxies and quasars in the redshift range $0.001 < z < 3$ [23]. In figure 3.4-3 (a) the observation data is set between two Euclidean lines of the DU prediction in Table 3.4-II(3). The FLRW prediction is calculated for the conventional Einstein de Sitter case (Ω_m= 1 and Ω_Λ= 0) shown by the solid curve, and for the recently preferred case with a share of dark energy included as Ω_m= 0.27 and Ω_Λ = 0.73 (dashed curves). Both FLRW predictions deviate significantly from the Euclidean lines in (a), that enclose the set of data uniformly in the whole redshift range observed. As shown in figure 3.4-3 (b) the effect of the dark energy contribution on the FLRW prediction of the angular size is marginal.

Figure 3.4-4 compares the predictions for the *K*-corrected magnitudes of Ia supernovae in DU and FLRW space, respectively. The observed magnitudes in the figure are based on Riess et al.'s "high-confidence" dataset and the data from the HST [24]. See Appendix A1 for a detailed analysis.

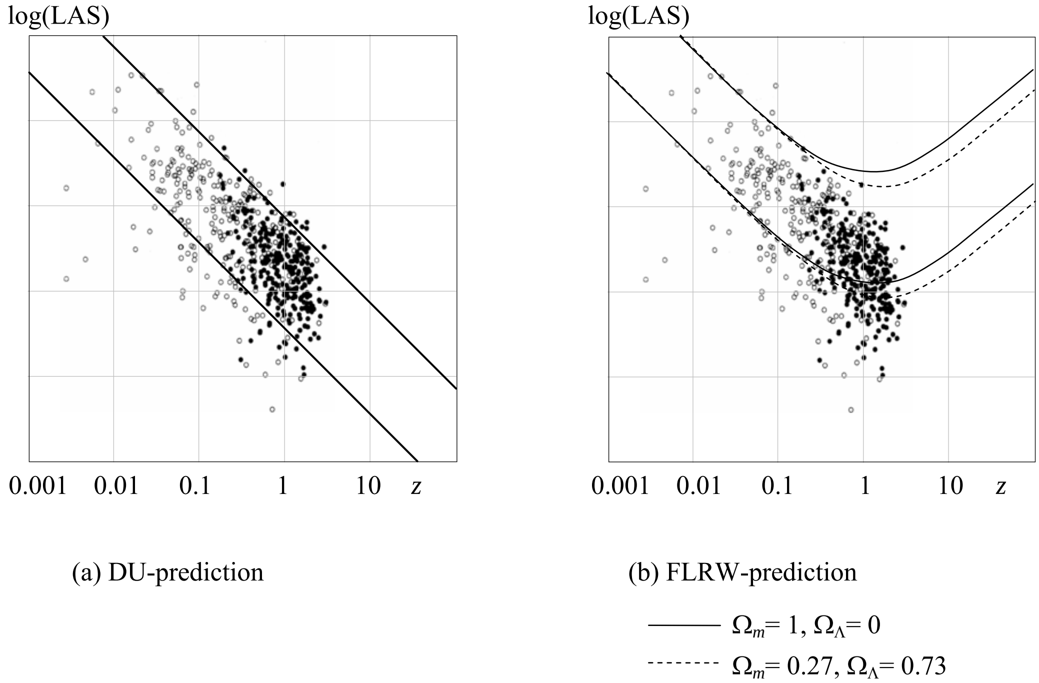

Figure 3.4-3. Dataset of observed Largest Angular Size (LAS) of quasars and galaxies in the redshift range $0.001 < z < 3$ which is the range achievable with todays' techniques. Open circles are galaxies, filled circles are quasars [23]. In (a) observations are compared with the DU prediction [Table 3.4-2(3)]. In (b) observations are compared with the FLRW prediction [Table 3.4-2(3)] with Ω_m= 0 and Ω_Λ = 0 (solid curves), and Ω_m= 0.27 and Ω_Λ= 0.73 (dashed curves).

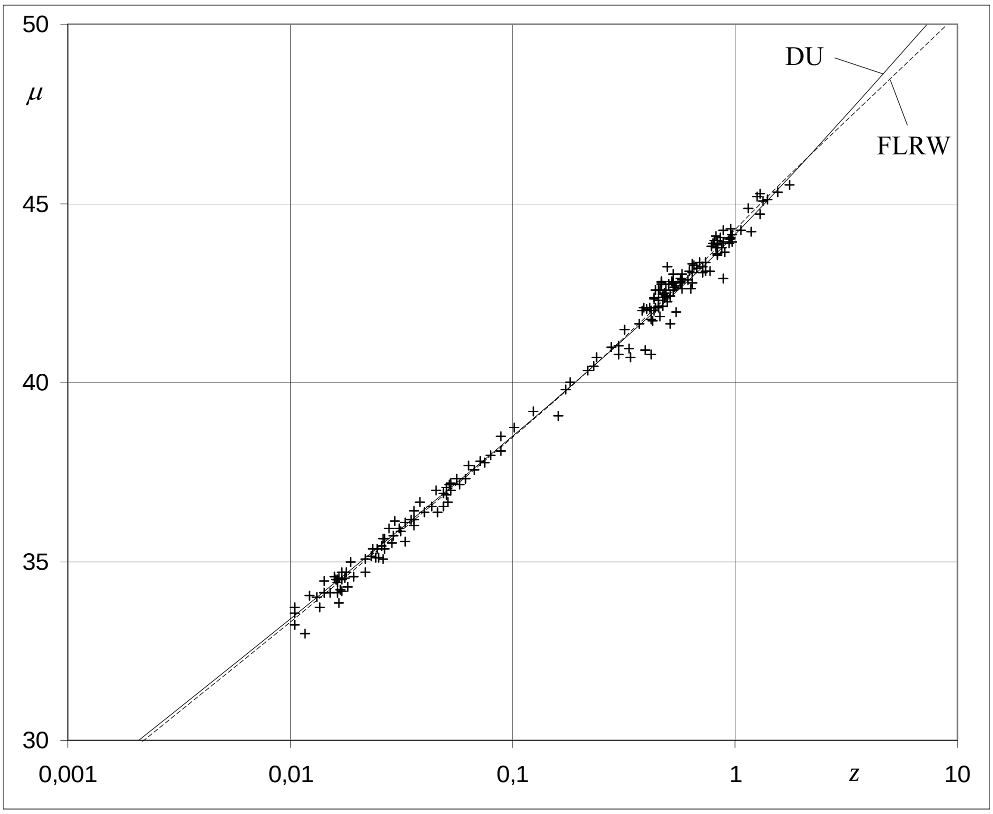

Figure 3.4-4. Distance modulus $\mu = m - M$, vs. redshift for Riess et al. "high-confidence" dataset and the data from the HST for Ia supernovae, Riess [24]. The optimum fit for the FLRW prediction is based on Ω_m 0 0.27 and Ω_Λ = 0.73. In spite of the essentially different derivation and mathematical appearance [see Table 3.4-II(5)] the difference between the DU prediction [see Table 3.4-II(5)] (solid curve), and the prediction of the standard model (dashed curve) is very small in the red-shift range covered by observations, but becomes meaningful at redshifts above $z > 3$. Unlike the FLRW prediction, the DU prediction has no adjustable parameters.

4. Summary and conclusions

Dynamic Universe is holistic approach to the description of physical reality. Space is studied as a closed energy system manifested by the dynamics resulting from the zero-energy balance of motion and gravitation in the structure. Relativity in such a structure is not relativity between the observer and the object but global relativity between local and the whole. Global relativity is not described in terms of modified coordinate quantities. Time and distance in DU space are universal. Global relativity shows the locally available share of total energy in space via a system of nested energy frames relating the locally available rest energy of an object to the rest energy the object had at rest in hypothetical homogeneous space where all mass is uniformly distributed into space.

The DU approach shows the role of mass as wavelike substance for the expression of energy and allows a unified expression of all energy forms. The identification of a common substance paves the way towards a unified picture of physics including the quantum mechanical description of local energy structures. In the DU perspective unification is not searched from the unification of forces but from a unified description of energy and the unbroken linkage of energy structures from elementary particles up to whole space — or perhaps more correctly, from whole space down to the multitude of local structures. The linkage of local and whole is complemented by the overall zero-energy balance of the rest energy and the global gravitational energy which provides a negative counterpart to the rest energy of a local object.

The DU approach leads to a compact description of the structure and development of space describable largely in a closed mathematical form which provides precise predictions to physical and cosmological observables in an excellent agreement with observations.

Acknowledgements

The author expresses his sincere thanks to Ari Lehto, Heikki Sipilä, and Tarja Kallio-Tamminen for many insightful discussions on the laws of nature, the philosophy of physics, and the theoretical basis of the Dynamic Universe model behind this paper.

References

1. R. Feynman, W. Morinigo, and W. Wagner, Feynman Lectures on Gravitation (during the academic year 1962-63), Addison-Wesley Publishing Company, p. 10 (1995)
2. R. Feynman, W. Morinigo, and W. Wagner, Feynman Lectures on Gravitation (during the academic year 1962-63), Addison-Wesley Publishing Company, p. 164 (1995)
3. T. Suntola, "*Theoretical Basis of the Dynamic Universe*", ISBN 952-5502-1-04, Suntola Consulting Ltd., 292 pages, 2004. Summary of the book (pdf): www.physicsfoundations.org/society/library/2008_Introduction.pdf
4. T. Suntola and Robert Day, "*Supernova observations fit Einstein-deSitter expansion in 4-sphere*", arXiv/astro-ph/0412701 (2004)
5. T. Suntola, *"Back to the Basis – Observations Support Spherically Closed Dynamic Space"*, 1st Crisis in Cosmology Conference (CCC-1), Monção, Portugal, June 23-25, 2005, arXiv/astro-ph/0509016 (2005)
6. T. Suntola, "*Photon - the minimum dose of electromagnetic radiation*", in "*The Nature of light – What Is a Photon*?", Taylor & Francis Group, CRC Press, ISBN 978-1-4200-4424-9 (2008)
7. T. Suntola, *"Dynamic space converts relativity into absolute time and distance"*, PIRT-IX, "Physical Interpretations of Relativity Theory IX", London, September 3-9, 2004
8. T. Suntola, *"Relativity defines the locally available share of total energy"*, PIRT-X, "Physical Interpretations of Relativity Theory X", London, September 8-11, 2006
9. T. Suntola, *"Zero-energy space cancels the need for dark energy"*, Proceedings of PIRT Budapest 7-9.9.2007
10. G. W. Leibniz, *Matematischer Naturwissenschaflicher und Technischer Briefwechsel, Sechster band* (1694)
11. J. Foster, J. D. Nightingale, A Short Course in General Relativity, 2nd edition, Springer-Verlag, ISBN 0-387-94295-5 (2001)
12. R. Genzel, et al., Nature 425, 934 (2003)
13. The Mariner Mars missions, NASA http://nssdc.gsfc.nasa.gov/planetary/mars/mariner.html
14. C.W. Misner., K. S. Thorne & J.A. Wheeler, "Gravitation", W. H. Freeman & Co., New York (1973)
15. R. C. Tolman, PNAS 16, 511-520 (1930)
16. E. Hubble, M. L. Humason, Astrophys.J., 74, 43 (1931)
17. W. de Sitter, B.A..N., 7, No 261, 205 (1934)
18. E. Hubble and R. C. Tolman, ApJ, 82, 302 (1935)
19. E. Hubble, Astrophys. J., 84, 517 (1936)
20. H. P. Robertson, Zs.f.Ap., 15, 69 (1938)
21. S. M. Carroll, W. H. Press, and E. L. Turner, ARA&A, 30, 499 (1992)
22. A. Kim, A. Goobar, & S. Perlmutter, PASP, 190–201 (1996)
23. K. Nilsson et al., Astrophys. J., 413, 453, (1993)
24. A. G. Riess, et al., [Supernova Search Team Collaboration], Astron. J. 116, 1009 (1998)
25. A. G. Riess, et al., Astrophys. J., 607, 665 (2004)
26. A. G. Riess, et al., [arXiv:astro-ph/0611572] (2006)
27. S. Perlmutter, et al. [Supernova Cosmology Project Collaboration], Astrophys. J. 517, 565 (1999)
28. R. Knop, et al., ApJ, 598, 102 (2003)
29. J. T. Tonry, et al., ApJ, 594, 1 (2003)
30. B. Barris, et al., ApJ, 602, 571(2004)
31. P. Astier, et al. [Supernova Legacy Survey, SNLS]:A&A 447, 31–48 (2006)
32. A. Conley, et al., ApJ, 644, 1 (2006)
33. Sandage, A., Perelmuter, J-M., ApJ, 370, 455 (1991)
34. Tonry, J. T., et al., ApJ, 594, 1 (2003) [arXiv:astro-ph/0305008]
35. Sandage, A., ApJ, 133, 355-392 (1961)
36. Sandage, A., Perelmuter, J-M., ApJ, 350, 481-491 (1990)
37. Lubin, L.M. and Sandage, A., AJ, 121, 2271-2288 (2001a)
38. Lubin, L.M. and Sandage, A., AJ, 121, 2289-2300 (2001b)
39. Lubin, L.M. and Sandage, A., AJ, 122, 1071-1083 (2001c)
40. Lubin, L.M. and Sandage, A., AJ, 122, 1084-1103 (2001d)
41. Wilson, O.C., ApJ, 90, 634 (1939)
42. Roche, N., et al., Mon.Not.R.Astron.Soc. 293, 157-176 (1998)

Appendix 1. *Derivation of cosmological predictions*

A1.1 Optical distance and the Hubble law

As a consequence of the spherical symmetry and the zero-energy balance in space, the velocity of light is determined by the velocity of space in the fourth dimension. The momentum of electromagnetic radiation has the direction of propagation in space. Although the actual path of light is a spiral in four dimensions, the length of the optical path in the direction of the momentum of radiation in space, is the tangential component of the spiral, which is equal to the increase of the 4-radius, the radial component of the path, during the propagation, Fig. A1.1-1

$$D = R_0 - R_{0(0)} \qquad \text{(A1.1:1)}$$

The differential of optical distance can be expressed in terms of R_0 and the distance angle α as

$$dD = R_0 d\alpha = c_0 dt = dR_0 \qquad \text{(A1.1:2)}$$

By first solving for the distance angle α

$$\alpha = \int_{R_{0(0)}}^{R_0} \frac{dR_0}{R_0} = \ln\frac{R_0}{R_{0(0)}} = \ln\frac{R_0}{R_0 - D} \qquad \text{(A1.1:3)}$$

the optical distance D obtains the form

$$D = R_0\left(1 - e^{-\alpha}\right) \qquad \text{(A1.1:4)}$$

where R_0 means the value of the 4-radius at the time of the observation.

The observed recession velocity, the velocity at which the optical distance increases, obtains the form

$$v_{rec(optical)} = \frac{dD}{dt} = c_0\left(1 - e^{-\alpha}\right) = \frac{D}{R_0} c_0 \qquad \text{(A1.1:5)}$$

As demonstrated by equation (A1.1:5) the maximum value of the observed optical recession velocity never exceeds the velocity of light, c, at the time of the observation, but approaches it asymptotically when distance D approaches the length of 4-radius R_0.

Atoms conserve their dimensions in expanding space. As shown by Balmer's equation, the characteristic emission wavelength is directly proportional to the Bohr radius, which means that also the characteristic emission wavelengths of atoms are unchanged in the course of the expansion of space. The wavelength of radiation propagating in expanding space is assumed to be subject to increase in direct proportion to the expansion space, Fig. A1.1-1(b). Accordingly, redshift, the increase of the wavelength becomes

$$z = \frac{\lambda - \lambda_0}{\lambda_0} = \frac{R_0 - R_{0(0)}}{R_{0(0)}} = \frac{D/R_0}{1 - D/R_0} = e^{\alpha} - 1 \qquad \text{(A1.1:6)}$$

where $D = R_0 - R_{0(0)}$ is the optical distance of the object given in (A1.1:4), λ and R_0 are the wavelength and the 4-radius at the time of the observation, respectively, and $R_{0(0)}$ is the 4-radius of space at the time the observed light was emitted, see Fig. A1.1-1(b). Solved from (A1.1-6) the optical distance can be expressed

$$D = R_0 \frac{z}{1 + x} = R_0\left(e^{\alpha} - 1\right) \qquad \text{(A1.1:7)}$$

Space at redshift z is observed as the surface of an observer-centered 3-dimensional sphere with radius D, Fig. A1.1-1(c).

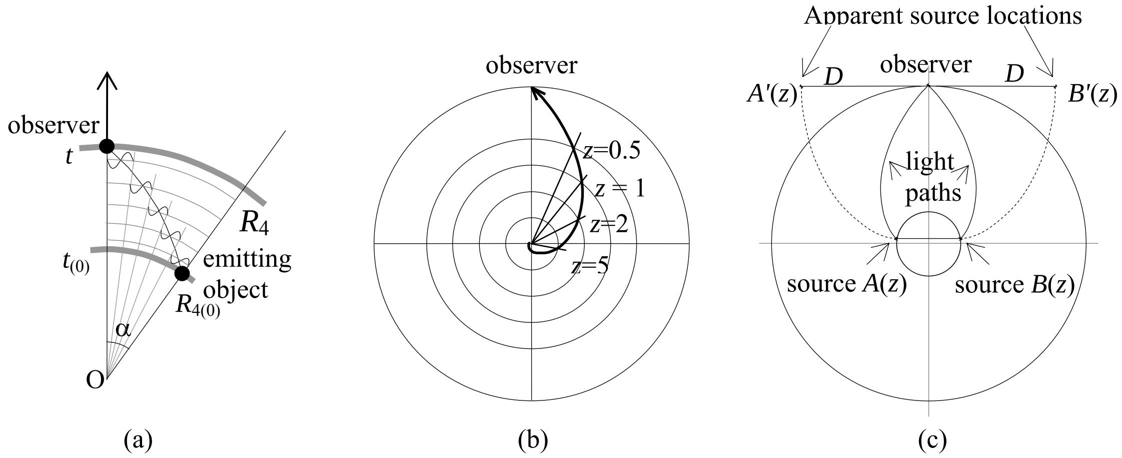

Figure A1.1-1. (a) The redshift of radiation results from the lengthening of the wavelength with the expansion of space. The number of quanta (or wavelengths of radiation) on the way from an emitter of constant intensity to an observer at a fixed distance angle from the emitter is constant with time. (b) Expansion of space during the propagation time of light from objects at different distances: The length of the 4-radius R_4 and the corresponding optical path is indicated for redshifts $z = 0.5$ to 5. (c) Propagation of light in expanding spherically closed space. The apparent line of sight is the straight tangential line. The distance to the apparent source of the light is at the optical distance $D = R_{(observation)} - R_{(emission)}$ along the apparent line of sight. Objects with redshift z, $A(z)$ and $B(z)$, are observed as apparent sources $A'(z)$ and $B'(z)$ on an observer centered 3-dimensional sphere with radius $D = R_0\, z/(1+z\,)$.

Atoms conserve their dimensions in expanding space. As shown by Balmer's equation, the characteristic emission wavelength is directly proportional to the Bohr radius, which means that also the characteristic emission wavelengths of atoms are unchanged in the course of the expansion of space. The wavelength of radiation propagating in expanding space is assumed to be subject to increase in direct proportion to the expansion space, Fig. A1.1-1(b). Accordingly, redshift, the increase of the wavelength becomes

$$z = \frac{\lambda - \lambda_0}{\lambda_0} = \frac{R_0 - R_{0(0)}}{R_{0(0)}} = \frac{D/R_0}{1 - D/R_0} = e^{\alpha} - 1 \qquad \text{(A1.1:6)}$$

where $D = R_0 - R_{0(0)}$ is the optical distance of the object given in (A1.1:4), λ and R_0 are the wavelength and the 4-radius at the time of the observation, respectively, and $R_{0(0)}$ is the 4-radius of space at the time the observed light was emitted, see Fig. A1.1-1(b). Solved from (A1.1-6) the optical distance can be expressed

$$D = R_0 \frac{z}{1+x} = R_0\left(e^{\alpha} - 1\right) \qquad \text{(A1.1:7)}$$

Space at redshift z is observed as the surface of an observer-centered 3-dimensional sphere with radius D, Fig. A1.1-1(c).

The optical distance D of equation (A1.1:7) corresponds closest to the angular diameter distance in the standard model [21]

$$D_A = \frac{R_H}{(1+z)} \int_0^z \frac{1}{\sqrt{(1+z)^2 (1+\Omega_m z) - z(2+z)\Omega_\Lambda}}\, dz \qquad \text{(A1.1:8)}$$

where the flat space condition, $\Omega_m + \Omega_\Lambda = 1$ is assumed, and $R_H = c/H_0$ is the Hubble radius corresponding to R_0 in DU space. Ω_m and Ω_Λ give the shares of the densities of baryonic plus dark mass and the dark energy in space, respectively. The term "angular diameter distance" refers to the distance converted into the observation angle of a standard rod and non-expanding objects in space. In FLRW cosmology not only solid objects like stars but also all local systems like galaxies and quasars are non-expanding objects which allows the expression of the observation angle of cosmological objects generally as

$$\theta = \frac{d}{D_A} = \frac{d}{R_H}(1+z) \Bigg/ \int_0^z \frac{1}{\sqrt{(1+z)^2 (1+\Omega_m z) - z(2+z)\Omega_\Lambda}}\, dz \qquad \text{(A1.1:9)}$$

The observation angle of a standard rod or *non-expanding objects* (solid objects like stars) in DU space is

$$\theta = \frac{d_{rod}}{D} = \frac{d_{rod}}{R_4}\frac{(1+z)}{z} \quad ; \quad \frac{\theta}{d_{rod}/R_4} = \frac{(1+z)}{z} \tag{A1.1:10}$$

As shown by equation (A1.1:10), the observation angle of a standard rod approaches the size angle $\alpha_d = d_{rod}/R_4$ of the object at high redshift ($z >> 1$).

In DU space gravitationally bound local systems expand in direct proportion to the expansion of space. The angular size of an *expanding object* with diameter $d = d_R/(1+z)$ at the time light from the object is emitted is

$$\theta = \frac{d}{D} = \frac{d_R}{(1+z)}\frac{(1+z)}{R_4 z} = \frac{d_R}{R_4}\frac{1}{z} = \frac{\alpha_d}{z} \quad ; \quad \frac{\theta}{R_4/d_R} = \frac{\theta}{\alpha_d} = \frac{1}{z} \tag{A1.1:11}$$

where the ratio $d_R/R_4 = \alpha_d$ means the angular size of the expanding object as seen from the center of the 4-sphere. Equation (A1.1:11) implies Euclidean appearance of expanding objects.

The standard model of FLRW space defines two other distance quantities related to the angular diameter distance. The *co-moving distance* is the distance of objects as it is at the time of observation, i.e. excluding the light propagation time from the object. The co-moving distance in the FLRW space is

$$D_{Co-moving} = (1+z)D_A = R_H \int_0^z \frac{1}{\sqrt{(1+z)^2(1+\Omega_m z) - z(2+z)\Omega_\Lambda}}dz \tag{A1.1:12}$$

The DU equivalence of co-moving distance is the physical distance measured along the curved surface of spherically closed space

$$D_{phys} = \alpha R_0 = R_0 \ln(1+z) \tag{A1.1:13}$$

Luminosity distance in FLRW space is the distance equivalence (in parsec) used to convert distance into *magnitude* using the classical definition of magnitude

$$M = m - 5\cdot\log(D_L - 1) \quad ; \quad D_L = 10^{\frac{(m-M)}{5}+1} \tag{A1.1:14}$$

or in a more illustrative form to give the apparent magnitude *m* in equation

$$m = M + 2.5\cdot\log\left[\left(\frac{R_H}{d_0}\right)^2\right] + 2.5\cdot\log\left[\left(\frac{D_L}{R_H}\right)^2\right] \tag{A1.1:15}$$

where *M* is the absolute magnitude of the reference source at distance d_0 = 10 pc. The Luminosity distance in FLRW cosmology is

$$D_L = (1+z)^2 D_A = R_H(1+z)\int_0^z \frac{1}{\sqrt{(1+z)^2(1+\Omega_m z) - z(2+z)\Omega_\Lambda}}dz \tag{A1.1:16}$$

which assumes factor $(1+z)^2$ for the redshift dilution in the observed power density (see section A1.2) and another $(1+z)^2$ "aberration factor" for the spreading of radiation due to expansion. The magnitude prediction based on luminosity distance D_L in FLRW cosmology assumes reduction of the observed power densities to power densities in "emitter's rest frame" by a (1+z) factor in the *K-correction* which is classically used as the instrumental correction for redshifted spectrum, see sections A1.3 and A1.4.

In DU space the dilution factor of redshift is (1+z). In DU space, luminosity distance for observed bolometric power density is

$$D_{L(DU)} = D\sqrt{1+z} = R_0\cdot\frac{z}{1+z}\sqrt{1+z} = R_0\cdot z\sqrt{1+z} \tag{A1.1:18}$$

The physical basis of the redshift dilution is discussed in section A1.2. Figure A1.1-2 compares the distance definitions in FLRW space and DU space.

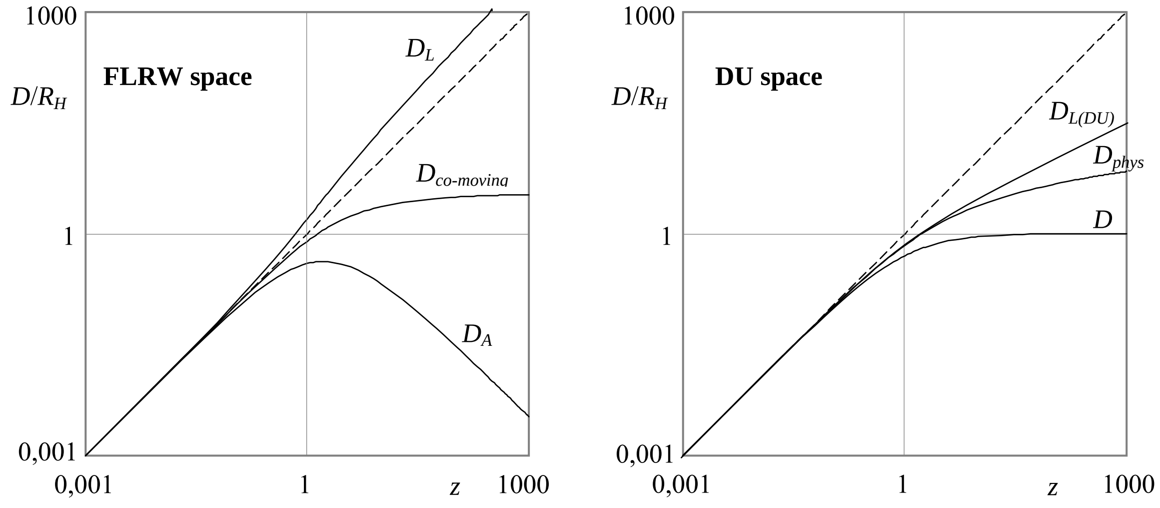

Distances in FLRW space:
a) Luminosity distance, D_L
b) Co-moving distance, $D_{co\text{-}moving}$
c) Angular diameter distance, D_A

Distances in DU space:
a) Luminosity distance, $D_{L(DU)}$
b) Physical distance, D_{phys}
c) Optical distance, D

Figure A1.1-2. Comparison of distance definitions in FLRW space and DU space. The dashed line in both figures is the linear distance corresponding to classical Hubble law $D = H_0 z$.

A1.2 The effects of redshift and distance on electromagnetic radiation

In the DU framework the Coulomb energy and the energy of electromagnetic radiation can be expressed in terms of a mass equivalence and the velocity of light, formally, like the rest energy of matter.

Matter: $$E_{rest} = mc_0 c \qquad \text{(A1.2:1)}$$

Cycle (N^2 quanta) of electromagnetic radiation: $$E_\lambda = N^2 \frac{h_0}{\lambda_e} c_0 c = m_\lambda c_0 c \qquad \text{(A1.2:2)}$$

Coulomb energy: $$E_C = N_1 N_2 \alpha \frac{h_0}{2\pi r} c_0 c = m_C c_0 c \qquad \text{(A1.2:3)}$$

Conserving the mass equivalence of a quantum of radiation, the energy flux of electromagnetic radiation becomes

$$F_{rec} = E_\lambda f = \frac{h_0}{\lambda_e} cc_0 \cdot f = \frac{h_0}{\lambda_e} \frac{c_0 c^2}{\lambda_e (1+z)} = \frac{h_0 c_0 c^2}{\lambda_e^2 (1+z)} \qquad \text{(A1.2:4)}$$

where λ_e is the wavelength of radiation at the emission. The reference flux emitted by an identical source at the time and location the redshifted radiation is received ($\lambda_r = \lambda_e$) is

$$F_{emit(ref)} = E_\lambda f = \frac{h_0}{\lambda_e} cc_0 f = m_{\lambda_e} cc_0 \frac{c}{\lambda_e} = \frac{h_0}{\lambda_e} \frac{c_0 c^2}{\lambda_e} = \frac{h_0 c_0 c^2}{\lambda_e^2} \qquad \text{(A1.2:5)}$$

Relative to the reference flux, the power density in the redshifted flux is

$$F_{rec} = \frac{F_{emit(ref)}}{(1+z)} \qquad \text{(A1.2:6)}$$

In DU space, the energy flux observed in radiation redshifted by z is diluted by factor (1+z), not by factor $(1+z)^2$ as assumed in the standard model solution [33]. The difference comes from the interpretation of the effect of redshift on the energy of a quantum. As first proposed by Hubble and Humason [16] and later by de Sitter [17], the energy of a quantum is reduced by (1+z) as a consequence of the effect of Planck's equation $E = hf$ as a reduction of the "intensity of the radiation". When receiving the redshifted radiation at a lowered frequency, a second (1+z) factor was assumed. Hubble [19] considered that the latter is relevant only in the case that the redshift is due to recession velocity [18]. The first (1+z) factor was called the "energy effect" and the second (1+z) factor the "number effect".

Conservation of the mass equivalence of radiation in DU space negates the basis for an "energy effect" as a violation of the conservation of energy. An analysis of the linkage between Planck's equation and Maxwell's equations shows that Planck's equation describes the energy conversion at the *emission* of electromagnetic radiation. Redshift should be understood as *dilution of the energy density due to an increase in the wavelength* in the direction of propagation, not as *losing of energy*. Accordingly, the observed energy flux $F = E_\lambda f$ is subject only to a single (1+z) dilution factor, the "number effect" in the historical terms.

Referring to equation (A1.2:4), at distance D from source A the density of the energy flux F_A is

$$F_A = \frac{N^2}{4\pi D^2} \frac{h_0 c_0 c^2}{\lambda_e^2 (1+z)} \tag{A1.2:7}$$

where N is the intensity factor of the source. Related to the flux density F_B from a reference source B with same intensity at distance d_0 ($z \approx 0$) the energy flux F_A is

$$F_A = F_B \cdot \frac{N^2}{4\pi D^2} \frac{h_0 c_0 c^2}{\lambda_e^2 (1+z)} \Bigg/ \frac{N^2}{4\pi d_0^2} \frac{h_0 c_0 c^2}{\lambda_e^2} = F_B \cdot \frac{d_0^2}{D^2} \frac{1}{(1+z)} \tag{A1.2:8}$$

Substitution of equation (A1.1:7) for D in (A1.2:8) gives

$$F_A = F_B \cdot \frac{d_0^2}{R_4^2} \frac{(1+z)^2}{z^2} \frac{1}{(1+z)} = F_B \cdot \frac{d_0^2}{R_4^2} \frac{(1+z)}{z^2} \tag{A1.2:9}$$

For a d_0 = 10 pc reference source, $F_B = F_{10pc}$ we get the expression for the apparent magnitude

$$m = M - 2.5 \log \frac{F_A}{F_{10pc}} = M + 5 \log \frac{R_4}{d_0} + 5 \log z - 2.5 \log(1+z) \tag{A1.2:10}$$

where M is the absolute magnitude of the reference source at distance d_0.

Equation (A1.2:10) applies for the *bolometric energy flux* observed for radiation from a source at optical distance (angular size distance) $D = R_4 \cdot z / (1+z)$ from the observer in DU space. Equation (A1.2:10) does not include possible effects of galactic extinction, spectral distortion in Earth atmosphere, or effects due to the local motion and gravitational environment of the source and the receiver.

In the present practice, apparent magnitudes are expressed as *K*-corrected magnitudes which in addition to instrumental factors for bolometric magnitude include a "correction to source rest frame" required by the prediction of the apparent magnitude in the standard cosmology model. To make the DU prediction in equation (A1.2:10) consistent with the *K*-corrected magnitudes assumed in the FLRW prediction, equation (A1.2:10) is be complemented as

$$m_{(K)} = M + 5 \log \frac{R_4}{D_0} + 5 \log z - 2.5 \log(1+z) + K \tag{A1.2:11}$$

The *K*-correction is discussed in detail in section A1.4.

A1.3 Multi-bandpass detection

For analyzing the detection of bolometric flux densities and magnitudes by multi-bandpass photometry the source radiation is assumed to have the spectrum of blackbody radiation. The bandpass system applied consists of a set of UBVIZYJHK filters approximated with transmissions curves of the form of normal distribution

$$f_X(\lambda) = e^{-\left[(\lambda - \lambda_{0X})^2 / 2(\Delta\lambda_X / \sigma_{1/2})^2\right]} = e^{-\frac{\sigma_{1/2}^2}{2} \frac{\lambda_{C(X)}}{\Delta\lambda_X} \left(\frac{\lambda}{\lambda_{C(X)}} - 1\right)^2} = e^{-\frac{2.773}{W_X^2} \left(\frac{\lambda}{\lambda_{C(X)}} - 1\right)^2} \tag{A1.3:1}$$

where $\lambda_{C(X)}$ is the peak wavelength of filter X, $\Delta\lambda_X$ the half width of the filter, $W_X = \Delta\lambda_X / \lambda_{C(X)}$ the relative width, and $\sigma_{1/2}$ = 2.35481 is half width deviation of the normal distribution (Fig. A1.3-1).

For the numerical calculation of the energy flux from a blackbody source, equation (A.2:10) in Appendix A2 is rewritten for a relative wavelength-differential $d\lambda_z/\lambda_z = d\lambda/\lambda << W_X$

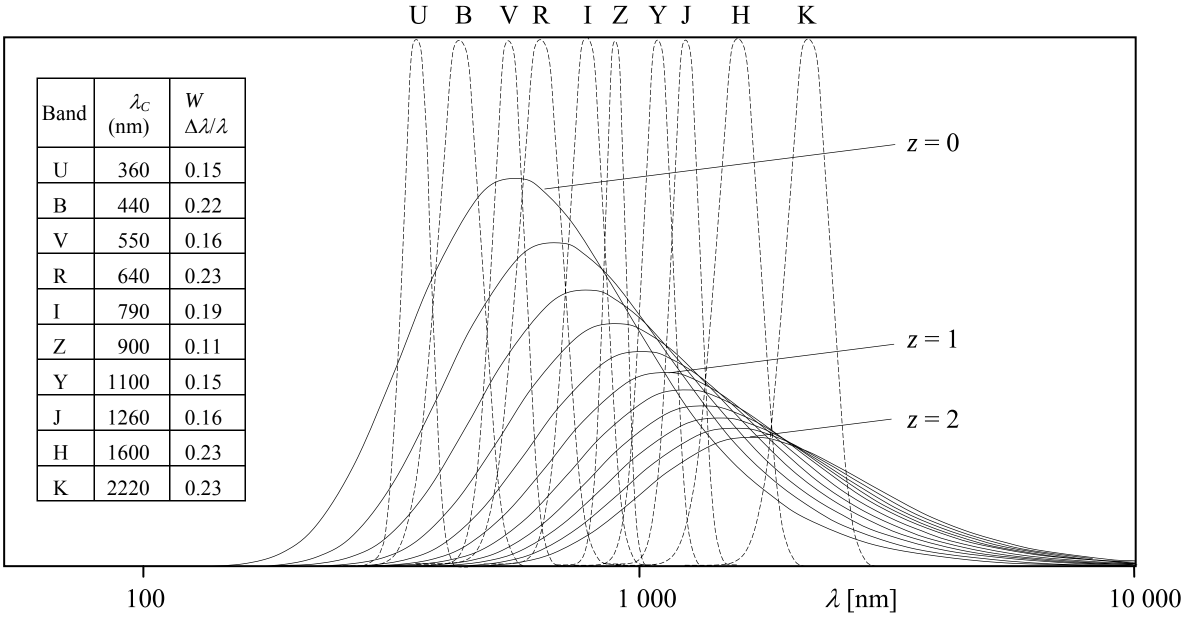

Figure A1.3-1. The effect of redshift z = 0…2 (shown in steps of 0.2) on the energy flux density per relative bandwidth of the blackbody radiation spectrum from a T = 6600 °K blackbody source corresponding to λ_T = 440 nm and λ_W = 557 nm (solid curves). Transmission curves of UBVRIZYJHK filters listed in the table are shown with dashed lines. The half widths of the filters follow the widths of standard filters in the Johnson system. All transmission curves are approximated with a normal distribution. The horizontal axis shows the wavelength in nanometers in a logarithmic scale.

$$F\left(\frac{d\lambda_z}{\lambda_z}\right) = \frac{15}{\pi^4}\frac{F_{bol(z=0)}}{(1+z)}\left[\left(\lambda_0\Big/\frac{\lambda}{1+z}\right)^4 \Big/ \left(e^{\left(\lambda_0/\frac{\lambda}{1+z}\right)}-1\right)\right]\frac{d\lambda}{\lambda} \qquad \text{(A1.3:2)}$$

Equation (A1.3:2) excludes the dilution due to the distance from the source to the observer. Integration of (A1.3:2) gives the bolometric radiation

$$F_{bol} = \int_0^\infty F\left(\frac{d\lambda_z}{\lambda_z}\right) = \frac{F_{bol(z=0)}}{1+z} \qquad \text{(A1.3:3)}$$

The transmission through filter X, normalized to the bolometric flux by applying equation (A2:12), can now be calculated by applying the transmission function of equation (A1.3:1) to the flux in (A1.3:2)

$$dF_{X(z)}\left(\frac{d\lambda_z}{\lambda_z}\right) = \frac{1}{4.780}\frac{F_{bol(z=0)}}{(1+z)}\int_0^\infty\left[\left(\lambda_0\Big/\frac{\lambda}{1+z}\right)^4 \Big/ \left(e^{\left(\lambda_0/\frac{\lambda}{1+z}\right)}-1\right)\right] e^{-\frac{2.773}{W_X^2}\left(\frac{\lambda/(1+z)}{\lambda_{C(X)}}-1\right)^2}\frac{d\lambda}{\lambda} \qquad \text{(A1.3:4)}$$

which gives the flux observed through filter X as a function of the redshift of the radiation. Figure A1.3-2 shows the normalized transmission curves calculated for filters UBVRIZJ by integration of (A1.3:4). Each curve touches the bolometric curve (A1.3:3) at the redshift matching the maximum of the radiation flux to the nominal wavelength of the filter.

The energy flux of equation (A1.3:4) from sources at a small distance d_0 ($z_{do} \approx 0$) and at distance D (z_D > 0) are related

$$\frac{F_{X(D)}}{F_{X0(d_0)}} = \frac{d_0^2}{D^2}\frac{\int_0^\infty dF_{X(z)}}{\int_0^\infty dF_{X0(0)}} \qquad \text{(A1.3:5)}$$

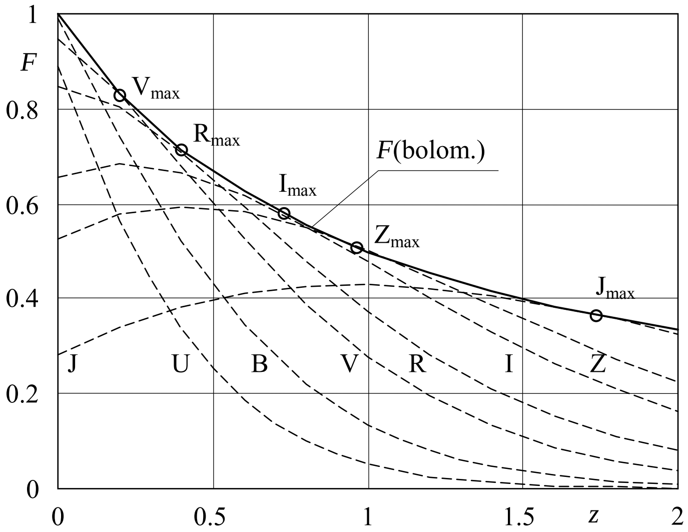

Figure A1.3-2. Transmission curves obtained by numerical integration of (58) for filters UBVRIZJ for radiation in the redshift range $z = 0\ldots2$ from a blackbody with $\lambda_T = 350$ nm ($\lambda_W = 440$ nm, $T = 8300$ °K). Each curve touches the bolometric curve of equation (57) at the redshift matching maximum of the radiation flux to the nominal wavelength λ_W of the filter (small circles in the figure).

Substitution of equation (A1.1:7) for D and equation (A1.3:4) for $F_{X(D)}$ and $F_{X0(do)}$ in (A1.3:5) gives the radiation power observed in filters X and $X0$ from standard sources at distances D and d_0, respectively

$$\frac{F_{X1(D)}}{F_{X2(d_0)}} = \frac{d_0^2}{R_4^2}\frac{(1+z)^2}{z^2}\frac{1}{(1+z)}\frac{\int_0^\infty \left[\left(\lambda_0 \Big/ \frac{\lambda}{1+z}\right)^4 \Big/ \left(e^{\left(\lambda_0 / \frac{\lambda}{1+z}\right)}-1\right)\right] e^{-\frac{2.773}{W_{X1}^2}\left(\frac{\lambda/1+z}{\lambda_{C(X1)}}-1\right)^2}\frac{d\lambda}{\lambda}}{\int_0^\infty \left[(\lambda_0/\lambda)^4 \Big/ \left(e^{(\lambda_0/\lambda)}-1\right)\right] e^{-\frac{2.773}{W_{X2}^2}\left(\frac{\lambda}{\lambda_{C(X2)}}-1\right)^2}\frac{d\lambda}{\lambda}} \qquad \text{(A1.3:6)}$$

By denoting the integrals in the numerator and denominator in (A1.3:6) by $I_{X(D)}$ and $I_{X0(do)}$, respectively, energy flux $F_{X(D)}$ can be expressed

$$F_{X(D)} = F_{X0(d_0)}\frac{d_0^2}{R_4^2}\frac{(1+z)}{z^2}\frac{I_{X(D)}}{I_{X0(d_0)}} \qquad \text{(A1.3:7)}$$

Choosing $d_0 = 10$ pc, the apparent magnitude for flux through filter X at distance D can be expressed as

$$m_{X1} = M + 5\log\left(\frac{R_4}{10\text{pc}}\right) + 5\log(z) - 2.5\log(1+z) + 2.5\log\left(\frac{I_{X2(d_0)}}{I_{X1(D)}}\right) \qquad \text{(A1.3:8)}$$

where M is the absolute magnitude of the reference source at distance 10 pc.

For $R_4 = 14\cdot10^9$ l.y., consistent with Hubble constant $H_0 = 70$ [(km/s)/Mpc], the numerical value of the second term in (A1.3:8) is $5\cdot\log(R_4/10\text{pc}) = 43.16$ magnitude units. For Ia supernovae the numerical value for the absolute magnitude is about $M \approx 19.5$.

When filter X is chosen to match $\lambda_{C(X)} = \lambda_W(1+z)$ and $\lambda_{C(X0)} = \lambda_W$ [or $\lambda_{C(X)} = \lambda_T(1+z)$ and $\lambda_{C(X0)} = \lambda_T$], the integrals $I_{X(D)}$ and $I_{X0(do)}$ are related as the relative bandwidths

$$\frac{I_{X0(d_0)}}{I_{X(D)}} = \frac{W_{X0}}{W_X} \qquad \text{(A1.3:9)}$$

which means that for optimally chosen filters with equal relative widths the last term in equation (A1.3:8) is zero and equation (A1.3:8) obtains the form of equation (A1.2:10) for bolometric energy flux

$$m_{X(opt)} = M + 5\log\left(\frac{R_4}{10\text{pc}}\right) + 5\log(z) - 2.5\log(1+z) \qquad \text{(A1.3:10)}$$

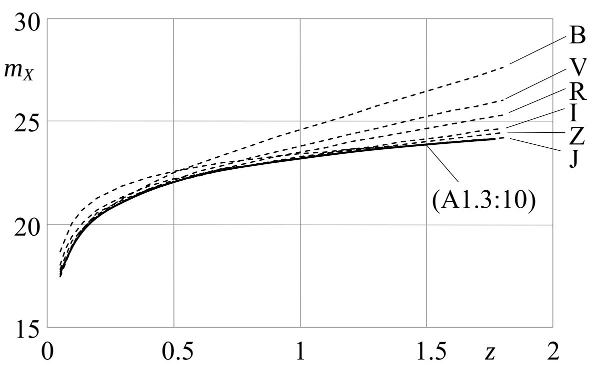

(a) λ_T = 350 nm (λ_W = 440 nm, T = 8300 °K)

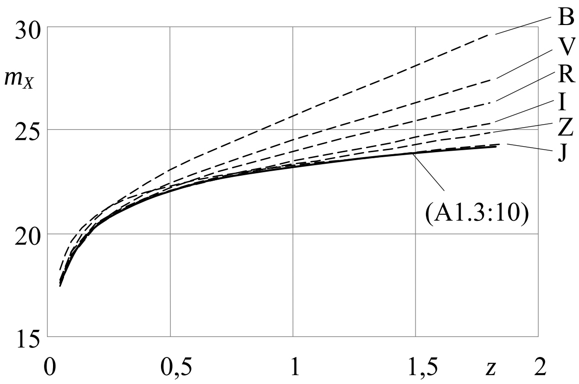

(b) λ_T = 440 nm (λ_W = 560 nm, T = 6600 °K)

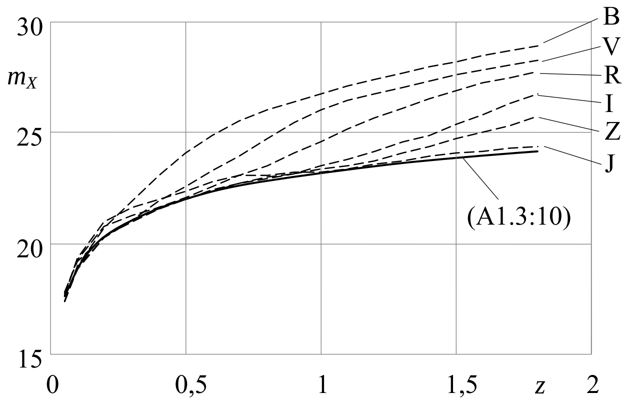

(c) Observed magnitudes Tonry et al., [34] Table 14.

Figure A1.3-3 (a, b) Predicted magnitudes (A1.3:8) for filters BVRIZJ as functions of redshift are shown as the families of curves drawn with dashed line. The blackbody temperature in (a) is 8300 °K and 6600 °K in (b), see Appendix A2 for the definitions of λ_T and λ_W characterizing blackbody radiation. (c) Plot of the peak magnitudes of normal Sn Ia observed in BVRIYJ filters as presented by Tonry et al. [34] in Table 14. The transmission functions of the filters used by Tonry et al. are slightly different from the transmission functions used in calculations for (a) and (b). The DU prediction (A1.3:10) for the magnitudes in optimally chosen filters is shown by the solid DU curve in each figure.

Figure A1.3-3 illustrates magnitudes calculated for filters *X = B, V, R, I, Z, J* from equation (A1.3:8) in the redshift range *z* = 0…2. Each curve touches the solid curve of equation (A1.3:10) corresponding to the bolometric magnitude obtainable with optimal filters at each redshift in the redshift range studied. The predictions are compared to observed magnitudes, Tonry et al. [34], Fig. A1.3-3(c).

A1.4 K-corrected magnitudes

In the observation praxis based on Standard Cosmology Model, direct observations of magnitudes in the bandpass filters are treated with *K-correction* which corrects the filter mismatch and converts the observed magnitude to the "emitter's rest frame" presented by observations in a bandpass matched to a low redshift reference of the objects studied. The *K-correction* for observations in the X_j band relative to the rest frame reference in the X_i band is defined [22]

$$K_{i,j}(z) = 2.5\log(1+z) + 2.5\log\left\{ \frac{\int_0^\infty F(\lambda) S_i(\lambda)\, d\lambda \quad \int_0^\infty Z(\lambda) S_j(\lambda)\, d\lambda}{\int_0^\infty F\left(\lambda/(1+z)\right) S_j\, d\lambda \quad \int_0^\infty Z(\lambda) S_i(\lambda)\, d\lambda} \right\} \qquad \text{(A1.4:1)}$$

In the case of a blackbody source and filters with transmission functions described by a normal distribution, equation (A1.4:1) can be expressed by substituting equation (A1.3:2) for the energy flux integrals, equation (A1.3:1) for the transmission curves of the filters, and the relative bandwidths of filters *i* and *j* for the transmission integrals

$$K_{i,j(W)}(z) = 2.5\log(1+z)$$

$$+2.5\log\left\{ \frac{\int_0^\infty \left[(\lambda_0/\lambda)^5 \Big/ \left(e^{(\lambda_0/\lambda)} - 1\right) \right] e^{-\frac{2.773}{W_i^2}\left(\frac{\lambda}{\lambda_{C(i)}} - 1\right)^2} d\lambda}{\frac{1}{1+z}\int_0^\infty \left[\left(\lambda_0 \Big/ \frac{\lambda}{1+z}\right)^5 \Big/ \left(e^{\left(\lambda_0 / \frac{\lambda}{1+z}\right)} - 1\right) \right] e^{-\frac{2.773}{W_j^2}\left(\frac{\lambda/(1+z)}{\lambda_{C(j)}} - 1\right)^2} d\lambda} \frac{W_j}{W_i} \right\} \qquad \text{(A1.4:2)}$$

where the relative differential $d\lambda/\lambda$ of (A1.3:2) is replaced by differential $d\lambda$ to meet the definition of (A1.4:1). Figure A1.4-1 (a) illustrates the K_{BX}-corrections calculated for radiation from a blackbody source with $\lambda_T = 440$ nm equivalent to 6600 °K blackbody temperature. An optimal choice of filters, matching the central wavelength of the filter to the wavelength of the maximum of redshifted radiation, leads to the *K*-correction

$$K(z) \approx 5\log(1+z) \qquad \text{(A1.4:3)}$$

with an accuracy of better than 0.1 magnitude units in the whole range of redshifts covered with the set filters used. The difference between the *K*-corrections in equation (A1.4:2) and (A1.4:3) is presented in Figure A1.4-1(b).

Substitution of (A1.4:3) for *K* in equation (A1.2:11) gives the DU space prediction for *K*-corrected magnitudes

$$m_{X(opt)} = M + 5\log\frac{R_4}{D_0} + 5\log z + 2.5\log(1+z) \qquad \text{(A1.4:4)}$$

The prediction for *K*-corrected magnitudes in the standard model is given by equation

$$\begin{aligned} m &= M + 5\log\left(\frac{R_H}{10\text{ pc}}\right) + 5\log\left(\frac{D_L}{R_H}\right) \\ &= M + 43.2 + 5\log\left[(1+z)\int_0^z \frac{1}{\sqrt{(1+z)^2(1+\Omega_m z) - z(2+z)\Omega_\lambda}} dz\right] \end{aligned} \qquad \text{(A1.4:5)}$$

where $R_H = c/H_0 \approx 14 \cdot 10^9$ l.y. is the Hubble distance, the standard model replacement of R_4 in DU space, and D_L the luminosity distance defined in equation (A1.1:16). Mass density parameters Ω_m and Ω_Λ give the density shares of mass and dark energy in space. For a flat space condition the sum $\Omega_m + \Omega_\Lambda = 1$.

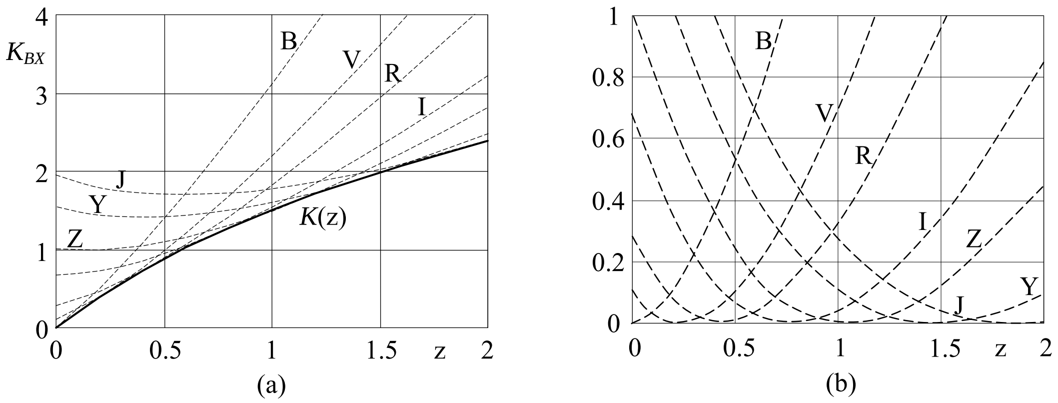

Figure A1.4-1. (a) K_{BX}-corrections (in magnitude units) according to (A1.4:2) for *B* band as the reference frame, calculated in the redshift range z = 0…2 for radiation from a blackbody source with λ_T =440 nm equivalent to 6600 °K blackbody temperature. All K_{BX}-correction curves touch the solid *K*(*z*) curve, which shows the *K*(*z*) = 5·log(1+*z*) function. (b) The difference K_{BX} –*K*(*z*). With an optimal choice of filters, the difference K_{BX} –*K*(*z*) is smaller than 0.05 magnitude units in the whole range of redshifts z = 0…2 covered by the set of filters B…J demonstrating the bolometric detection with optimally chosen filters.

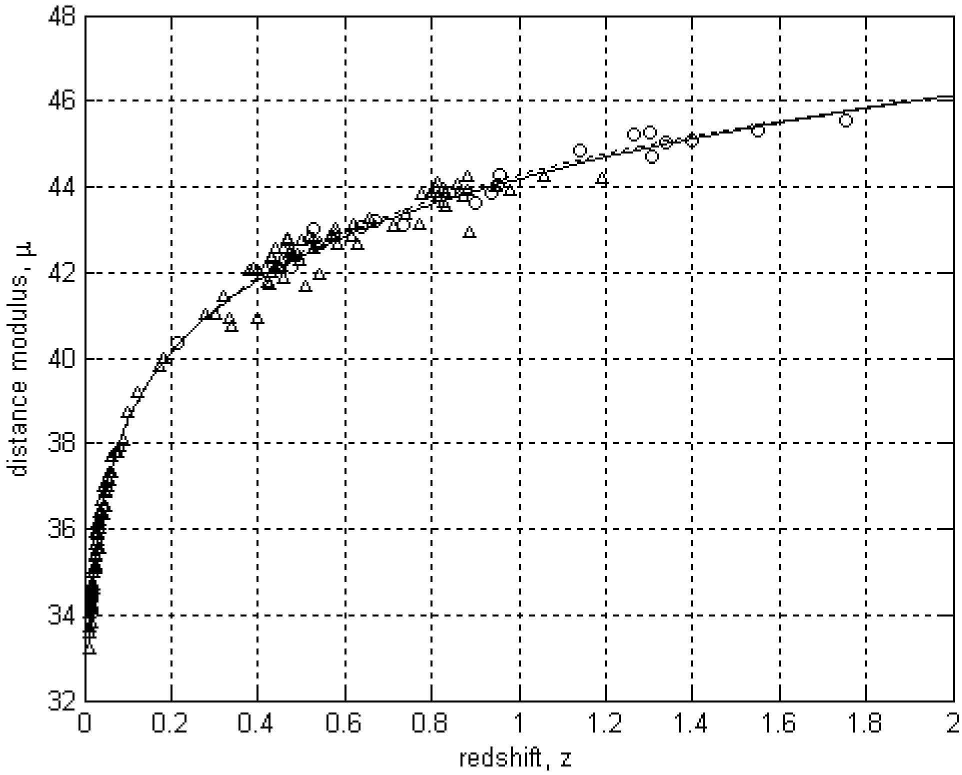

Figure A1.4-2. Distance modulus $\mu = m - M$, vs. redshift for Riess et al.'s gold dataset and the data from the HST. The triangles represent data obtained via ground-based observations, and the circles represent data obtained by the HST [24]. The optimum fit for the standard cosmology prediction (A1.4:5) is shown by the dashed curve, and the fit for the DU prediction (A1.4:4) is shown, slightly below, by the solid curve [4].

The best fit of equation (A1.4:5) to the *K*-corrected magnitudes of Ia supernova observations has been obtained with $\Omega_m = 0.26 \ldots 0.31$ and $\Omega_\Lambda = 0.74 \ldots 0.69$ [24…32]. Figure A1.4-2 shows a comparison of the prediction given by equation (A1.4:5) with $\Omega_m \approx 0.31$, $\Omega_\lambda \approx 0.69\ \Omega$ and $H_0 = 64.3$ used by Riess et al. [25] and the DU space prediction for *K*-corrected magnitudes in equation (A1.4:4).

In the redshift range $z = 0 \ldots 2$ the apparent magnitude of equation (A1.4:5) coincides accurately with the magnitudes of equation (A1.4:4). The *K*-corrections used by Riess et al. [25], Table 2, follow the $K(z) = 5 \cdot \log(1+z)$ prediction of equation (A1.4:3), Fig. A1.4-3.

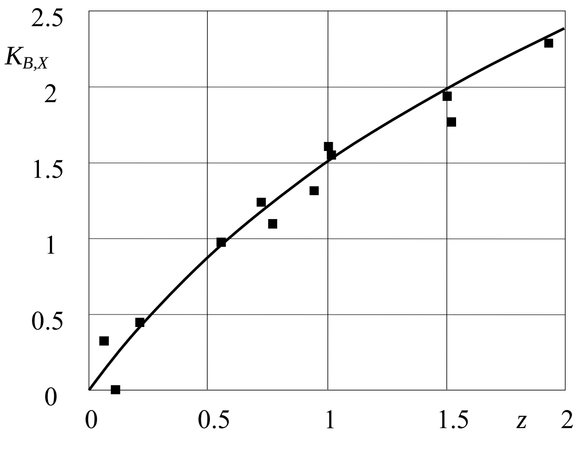

Figure A14-3. Average $K_{B,X}$-corrections (black squares) collected from the $K_{B,X}$ data in Table 2 used by Riess et al. (2004) for the *K*-corrected distance modulus data shown in Figure A1.4-2. The solid curve gives the theoretical *K*-correction (A1.4:3), $K = 5 \cdot \log(1+z)$, derived for filters matched to redshifted spectra (see Fig. A1.4-1) and applied in equation (A1.4:4) for the DU prediction for *K* corrected apparent magnitude.

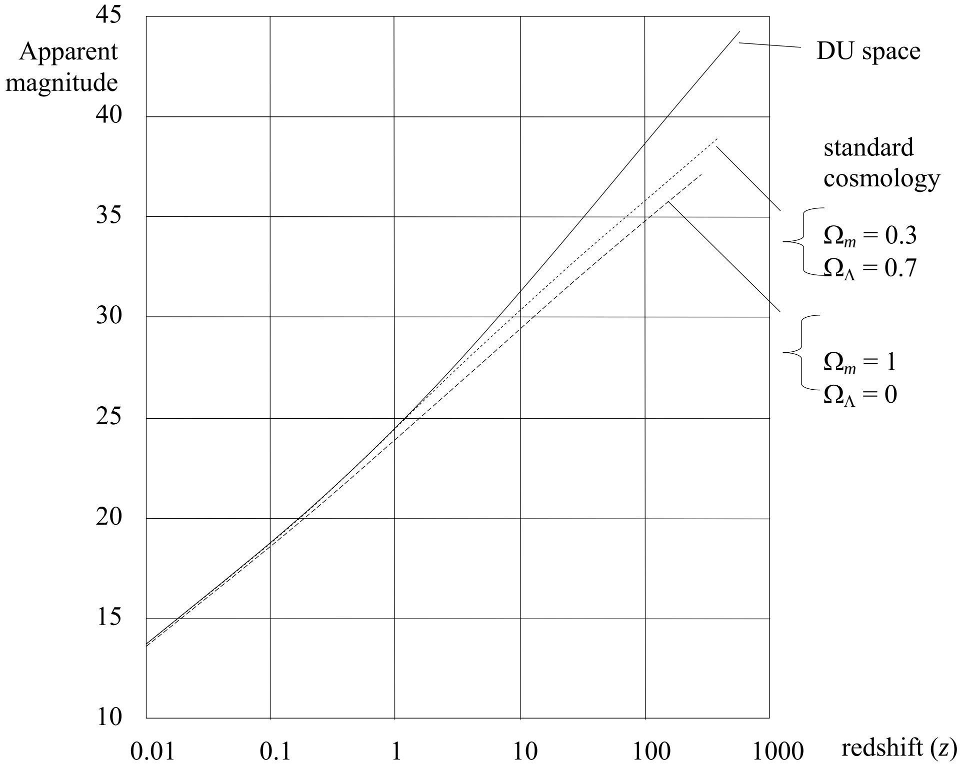

Figure A1.4-4. Comparison of predictions for the *K*-corrected apparent magnitude of standard sources in the redshift range 0.01...1000 given by the Standard Cosmology Model with Ω_m=0.3/Ω_Λ=0.7 and Ω_m=1/Ω_Λ=0 according to equation (A1.4:5), and DU space given by equation (A1.4:4). In each curve the absolute magnitude used is $M = -19.5$. The Ω_m=0.3/Ω_Λ=0.7 prediction follows the DU prediction closely up to redshift $z \approx 2$, the Ω_m=1/Ω_Λ=0 prediction of the standard model shows remarkable deviation even at smaller redshifts.

At redshifts above $z > 2$ the difference between the two predictions, (A1.4:4) and (A1.4:5), becomes noticeable and grows up to several magnitude units at $z > 10$, Fig. A1.4-4. For comparison, Figure A1.4-4 shows also the standard model prediction for $\Omega_m = 1$ and $\Omega_\lambda = 0$.

A1.5 Galaxy count

The relative volume differential dV/V of space as the function of the distance angle α from the observer is, Fig. A1.5-1,

$$\frac{dV}{V} = \frac{4\pi R_0^2 \sin^2\alpha \cdot R_0 d\alpha}{2\pi^2 R_0^3} = \frac{2\sin^2\alpha \cdot d\alpha}{\pi} = \frac{2/\pi \cdot \sin^2\left[\ln(1+z)\right]\cdot dz}{1+z} \qquad \text{(A1.5:1)}$$

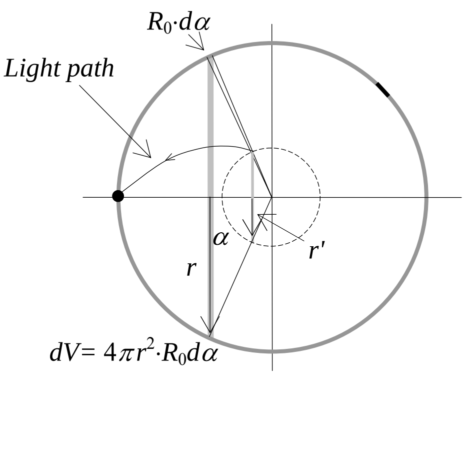

Figure A1.5-1. Calculation of the volume distribution as the function of distance angle α and redshift z. The relative share of dV of the total volume V of space is conserved throughout the expansion.

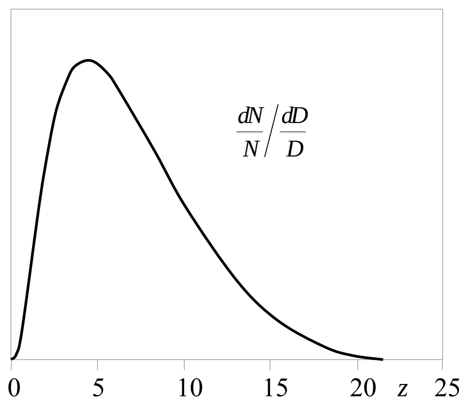

Figure A1.5-2. Number of galaxies in distance differential dD/D in redshift range 0…22, which corresponds to distance angle $\alpha = 0\ldots\pi/2$, i.e. across the spherically closed space. The calculated curve is based on a constant total number of galaxies in the redshift range studied.

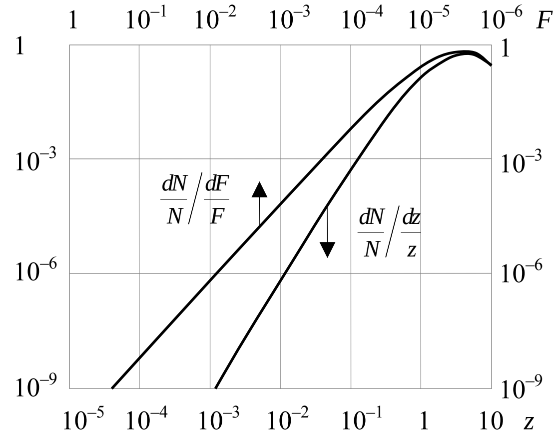

Figure A1.5-3. Prediction for the number of galaxies in redshift differential dz/z and in the observed bolometric power density differential dF/F in the redshift range $10^{-5}\ldots10$. Power density $F = 1$ at redshift $z = 10^{-5}$ has been chosen as the reference. The maximum number count /str occurs at redshift $z \approx 4.5$. No evolution factors are assumed in the prediction.

Assuming a constant number of galaxies in a redshift range studied, the number of galaxies can be related to a relative redshift differential, Fig. A1.1-2

$$\frac{dN}{N}\bigg/\frac{dz}{z} = \frac{dV}{V}\bigg/\frac{dz}{z} = \frac{2/\pi \cdot \sin^2\left[\ln\left(1+z\right)\right]\cdot z}{1+z} \qquad \text{(A1.5:2)}$$

and to the bolometric power density in a power range measured from the galaxies at different distances, Fig. A1.1-3

$$\frac{dN}{N}\bigg/\frac{dF}{F} = 2/\pi \cdot \sin^2\left[\ln\left(1+z\right)\right] \qquad \text{(A1.5:3)}$$

where the observed bolometric power density is inversely proportional to the square of distance D and diluted by factor (1+z) due to redshift z.

A1.6 Surface brightness of expanding and non-expanding objects

The Tolman test [18], [20], [35], and [36] is considered as a critical test for an expanding universe model. In expanding space, according to Tolman's prediction, the observed surface brightness of standard objects decreases by the factor $(1+z)^4$ with the redshift. Two of the four (1+z) factors are explained as consequences of the redshift on the radiation received: a decrease in the arrival rate (the number effect) and in the energy of photons (the energy effect), as discussed in Section A1.2. The two additional (1+z) factors are explained as an apparent increase in the observed area due to aberration.

With reference to equation (A1.1:11) the angular area of an expanding object like a galaxy with a present radius r_e is

$$\Omega_D = \left(\frac{r_{e(z)}}{D}\right)^2 = \frac{r_e^2}{\left(1+z\right)^2}\frac{\left(1+z\right)^2}{R_4^2 z^2} = \frac{r_e^2}{R_4^2}\frac{1}{z^2} \qquad \text{(A1.6:1)}$$

where D is the optical distance of the object. Accordingly, the observed bolometric surface brightness of the object is obtained by dividing the bolometric energy flux of equation (A1.2:9) by the angular size of equation (A1.6:1)

$$SB_{(D)} = \frac{F_D}{\Omega_D} = \frac{N^2}{2\pi}\frac{h_0 c_0 c^2}{\lambda_e^2\left(1+z\right)}\frac{\left(1+z\right)^2}{r_e^2} = \frac{N^2}{2\pi r_e^2}\frac{h_0 c_0 c^2\left(1+z\right)}{\lambda_e^2} \qquad \text{(A1.6:2)}$$

Compared to the surface brightness $SB_{(d_0)}$ of a reference object at distance d_0 with $z_{d_0} << 1$, the observed bolometric surface brightness $SB_{(D)}$ is

$$SB_{(D)} = SB_{(d_0)} \left(\frac{N^2}{2\pi r_e^2} \frac{h_0 c_0 c^2 (1+z)}{\lambda_e^2} \right) \Big/ \left(\frac{N^2}{2\pi r_e^2} \frac{h_0 c_0 c^2}{\lambda_e^2} \right) = SB_{(d_0)} (1+z) \quad \text{(A1.6:3)}$$

or related to the *K*-corrected energy fluxes in multi-bandpass system with nominal filter wavelengths matched to the redshifted radiation [see Section A1.4] as

$$SB_{K(D)} = SB_{(d_0)} (1+z)^{-1} \quad \text{(A1.6:4)}$$

The predictions of equations (A1.6:3) and (A1.6:4) do not include the effects of possible evolutionary factors.

In [37–40] Lubin and Sandage give a thorough review of the theoretical and observational aspects of the Tolman $(1+z)^{-4}$ surface brightness prediction as a test of the FLRW expansion. They conclude that observations of the light curves from supernovas have confirmed the cosmological time dilation [41] as a unique proof of an expanding space. They also interpret the precise Planckian shape of the background radiation as a solid proof of the Tolman surface brightness prediction. However, the observed surface brightnesses of high z objects do not follow the Tolman $(1+z)^{-4}$ prediction without assumptions of remarkable evolution in the luminosity and size of the objects.

Galaxy surface brightness and size analysis [42] of HST WFPC2 data in the redshift range $z = 0\ldots4$ shows a qualitative fit of observed surface brightnesses to equation (A1.6:4). Also, the observed reduction in the half-light radius with an increasing redshift is in line with the Euclidean appearance of galaxy space in the DU framework. A detailed analysis of the fit of surface brightness observations to predictions (A1.6:3) and (A1.6:4) is left outside the scope of this paper.

A1.7 The effects of the declining velocity of light

As a consequence of the conservation of the zero-energy condition assumed, all velocities in space are related to the velocity of light determined by the expansion in the direction of the 4-radius. Emission of quanta from a supernova explosion occurs at a frequency proportional to the velocity of light at the time of the explosion. A sequence of waves from an explosion is redshifted and accordingly received lengthened in the same ratio as the wavelengths are lengthened, i.e. in direct proportion to (1+z). In the standard model, the lengthening is referred to as cosmological time dilation, in DU space it is a direct consequence of reduced velocity of light at the time the wave sequence is received.

The declining rest energy of matter in DU space makes all atomic processes slow down with the expansion of space; ticking frequencies of atomic clocks and the rate of nuclear decay slow down in direct proportion to the decrease of the velocity of light. The present estimates for the oldest globular clusters, based on constant decay rates observed today, are in the range of 12 to 20 billion years [21].

The age of expanding DU space is $T = (2/3)\cdot R_4/c = (2/3)/H_0$ which means about 9.3 billion years for R_4 = 14 billion light years consistent with Hubble constant H_0 = 70 [(km/s)/Mpc]. Linear age estimates up to 14 billion years are reduced below the age of 9.3 billion years, Fig. A1.7-1.

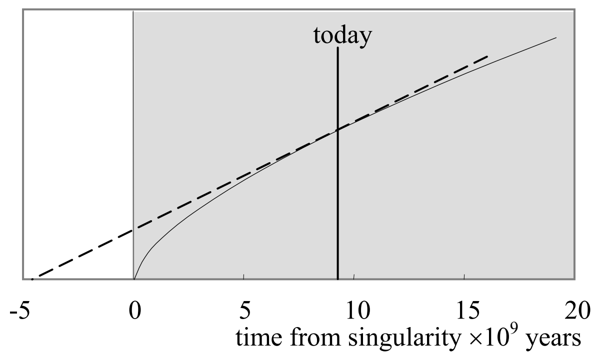

Figure A1.7-1. Accumulation of nuclear decay products at today's decay rate (dashed line), and at a rate proportional to the velocity of light in DU space (solid curve).

A1.8 Microwave Background radiation in DU space

The bolometric energy density of cosmic microwave background radiation, $4.2{\cdot}10^{-14}$ [J/m^3], corresponds, with a high accuracy, to the energy density *within a closed blackbody source* at 2.725 °K. (Obs. As indicated by the Stefan-Boltzmann constant, the energy density *within a blackbody source* is higher than the integrated energy density of the flux radiated by the source by a factor of 4.)

$$E_{bol(T=2.725\ °\mathrm{K})} = E_\nu d\nu = \int_0^\infty \frac{8\pi h}{c^3}\nu_0^3 \frac{\left(\nu/\nu_0\right)^3}{\left(e^{\nu/\nu_0}-1\right)} d\nu = 4.2\cdot 10^{-14} \quad \left[\frac{\mathrm{J}}{\mathrm{m}^3}\right] \qquad \text{(A1.8:1)}$$

where

$$\nu_0 \equiv \frac{kT}{h} = \frac{c}{\lambda_0} \qquad [\mathrm{Hz}] \qquad \text{(A1.8:2)}$$

from which $\nu_0 = 5.6910^{10}$ Hz is obtained for $T = 2.725$ °K.

The rest energy calculated for the total mass in space is $E_{rest} = M_\Sigma{\cdot}c^2 \approx 2{\cdot}10^{70}$ [J] corresponding to energy density $E_{rest}/(2\pi^2 R_4^3) = 4.6{\cdot}10^{-10}$ [J/m^3] in DU space. Assuming that CMB is equal everywhere in space, the share of the CMB energy density of the total energy density in space is about 10^{-4}. The total mass equivalence, and hence the ratio to the rest energy in space is conserved. The wavelength of radiation is redshifted as

$$z = \frac{R_4 - R_{4(e)}}{R_{4(e)}} = \frac{R_4}{R_{4(e)}} - 1 \qquad \text{(A1.8:3)}$$

where $R_{4(e)}$ is the 4-radius of space at the time of the emission of the CMB. The DU concept does not give a prediction for the value of the 4-radius $R_{4(e)}$ at the emission of the CMB — or exclude the possibility that the CMB were generated continuously by dark matter now at 2.725 °K, Fig. A1.8-1.

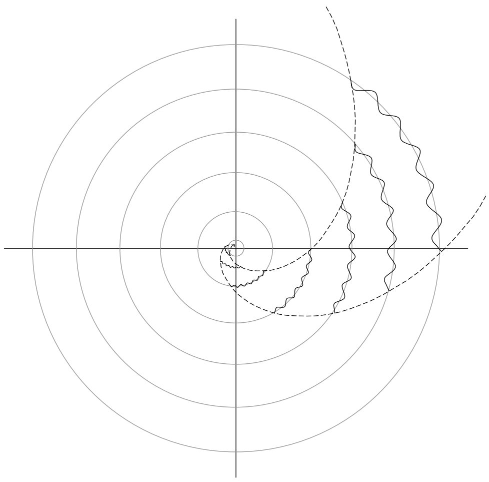

Figure A1.8-1. The CMB has the characteristics of a closed blackbody source. The number of quanta in radiation in spherically closed space is conserved. The wavelength, however, is increased in direct proportion to the expansion of the 4-radius. At present, the energy density of the 2.725 °K background radiation is about $4{\cdot}10^{-14}$ [J/m^3] which is about 0.01 % of the energy density of all mass in space.

*****

Appendix A2. *Blackbody radiation*

By denoting

$$\lambda_0 \equiv \frac{hc}{kT} \qquad \Rightarrow \quad \frac{\lambda_0}{\lambda} = \frac{hc}{\lambda kT} \quad ; \quad \lambda = \frac{hc}{kT}\frac{1}{\lambda_0/\lambda} \quad \text{and} \quad h\frac{c}{\lambda_0} = h\nu_0 = kT \tag{A2:1}$$

the energy density of a black body source expressed in terms of a wavelength differential $d\lambda$ is

$$dE_\lambda = E(\lambda)d\lambda = \frac{8\pi hc}{\lambda_0^5}\frac{(\lambda_0/\lambda)^5}{\left(e^{\lambda_0/\lambda}-1\right)}d\lambda \qquad \left[\frac{\mathrm{J}}{\mathrm{m}^3}\right] \tag{A2:2}$$

or in terms of a frequency differential $d\nu$

$$dE_\nu = E(\nu)d\nu = \frac{8\pi\nu_0^3 h}{c^3}\frac{(\nu/\nu_0)^3}{\left(e^{\nu/\nu_0}-1\right)}\cdot d\nu \qquad \left[\frac{\mathrm{J}}{\mathrm{m}^3}\right] \tag{A2:3}$$

The energy flux in terms of a wavelength differential $d\lambda$ or a frequency differential $d\nu$ from a black body source is obtained by multiplying the energy densities in (A2:2) and (A2:3) by the Stefan-Boltzmann factor $c/4$, and further divided by 4π for flux per steradian

$$\begin{aligned} dF_\lambda &= \frac{c}{4\cdot 4\pi}dE_\lambda = \frac{hc^2}{2\lambda_0^5}\frac{(\lambda_0/\lambda)^5}{\left(e^{\lambda_0/\lambda}-1\right)}d\lambda = F(\lambda)d\lambda \quad \left[\frac{\mathrm{W}}{\mathrm{m^2 sr}}\right] \\ F(\lambda) &= \frac{hc^2}{2\lambda_0^5}\frac{(\lambda_0/\lambda)^5}{\left(e^{\lambda_0/\lambda}-1\right)} = \frac{F_0}{\lambda_0}\frac{(\lambda_0/\lambda)^5}{\left(e^{\lambda_0/\lambda}-1\right)} \qquad \left[\frac{\mathrm{W}}{\mathrm{m^2 sr}}\Big/\mathrm{m}\right] \end{aligned} \tag{A2:4}$$

for equation (A2:2), and

$$\begin{aligned} dF_\nu &= \frac{c}{4\cdot 4\pi}dE_\nu = \frac{\nu_0^3 h}{2c^2}\frac{(\nu/\nu_0)^3}{\left(e^{\nu/\nu_0}-1\right)}d\nu = F(\nu)d\nu \left[\frac{\mathrm{W}}{\mathrm{m^2 sr}}\right] \\ F(\nu) &= \frac{\nu_0^3 h}{2c^2}\frac{(\nu/\nu_0)^3}{\left(e^{\nu/\nu_0}-1\right)} = \frac{F_0}{\nu_0}\frac{(\nu/\nu_0)^3}{\left(e^{\nu/\nu_0}-1\right)} \qquad \left[\frac{\mathrm{W}}{\mathrm{m^2 sr\,Hz}}\right] \end{aligned} \tag{A2:5}$$

for equation (A2:3). Factor F_0 in equations (A2:4) and (A2:5) is

$$F_0 = \frac{(kT)^4}{2c^2h^3} = \frac{h}{2}\frac{c^2}{\lambda_0^4} = \frac{h}{2}\frac{\nu_0^4}{c^2} \qquad \left[\frac{\mathrm{W}}{\mathrm{m^2 sr}}\right] \tag{A2:6}$$

The total energy flux from a black body source is obtained by integrating (A2:5) or (A2:6) for all wavelengths or frequencies. Substitution of $x = \lambda_0/\lambda$ in (A2:5) or $x = \nu/\nu_0$ in (A2:6) gives

$$F_{bol} = F_0\int_0^\infty \frac{x^3}{\left(e^x-1\right)}dx = \frac{\pi^4}{15}F_0 = \frac{\pi^4}{15}\frac{k^4T^4}{2c^2h^3} = \frac{\sigma}{4\pi}T^4 \quad \left[\frac{\mathrm{W}}{\mathrm{m^2 sr}}\right] \tag{A2:7}$$

where the numerical factor $\pi^4/15$ comes from the definite integral, T is the temperature of the black body source, and σ is the Stefan-Boltzmann constant $\sigma = 5.6693\cdot 10^{-8}$ [$\mathrm{Wm^{-2}{}^\circ K^{-4}}$].

The energy flux emitted in the wavelength or frequency range of a narrowband filter with relative width $W = W_\lambda = \Delta\lambda/\lambda = W_\nu = \Delta\nu/\nu$ is obtained from equations (A2:4) and (A2:5), respectively,

$$F_{W(\lambda)} = F_0 \frac{(\lambda_0/\lambda)^4}{\left(e^{\lambda_0/\lambda}-1\right)} \frac{d\lambda}{\lambda} = F_0 \frac{(\lambda_0/\lambda)^4}{\left(e^{\lambda_0/\lambda}-1\right)} W \quad \left[\frac{\mathrm{W}}{\mathrm{m^2 sr}}\right] \tag{A2:8}$$

$$F_{W(\nu)} = F_0 \frac{(\nu/\nu_0)^4}{\left(e^{\nu/\nu_0}-1\right)} \frac{d\nu}{\nu} = F_0 \frac{(\nu/\nu_0)^4}{\left(e^{\nu/\nu_0}-1\right)} W \quad \left[\frac{\mathrm{W}}{\mathrm{m^2 sr}}\right] \tag{A2:9}$$

or by relating the narrow band power density to the total bolometric flux density by expressing F_0 in terms of F_{bol} (A2:7) as

$$F_{W(\nu,\lambda)} = \frac{15}{\pi^4} \frac{(\nu/\nu_0)^4}{\left(e^{\nu/\nu_0}-1\right)} W \cdot F_{bol} = \frac{15}{\pi^4} \frac{(\lambda_0/\lambda)^4}{\left(e^{\lambda_0/\lambda}-1\right)} W \cdot F_{bol} \quad \left[\frac{\mathrm{W}}{\mathrm{m^2 sr}}\right] \tag{A2:10}$$

The distribution function $D = x^4/\left(e^x - 1\right)$ obtains its maximum value when $x = 3.9207$

$$D_{\max} = \left(\frac{x^4}{e^x - 1}\right)_{\max} = D_{(x=3.9207)} = 4.780 \tag{A2:11}$$

At a fixed relative bandwidth W the maximum flux occurs when the nominal frequency or wavelength of the filter $f_W = c/\lambda_W$ is $f_W/f_0 = \lambda_0/\lambda_W = 3.9207$

$$F_{W(\nu,\lambda)} = \frac{15}{\pi^4} \cdot D_{\max} \cdot W \cdot F_{bol} \quad \left[\frac{\mathrm{W}}{\mathrm{m^2 sr}}\right] \tag{A2:12}$$

which relates the energy flux through an ideal narrow band filter matched to the bolometric energy flux of the radiation. The nominal frequency of the filter is matched to the maximum power throughput of blackbody radiation by setting $f_W = 3.9207 \cdot f_0$.

When related to the frequency of the maximum power density per frequency f_T [W/Hz/m^2], and at the wavelength of the maximum power density per wavelength λ_T [W/m/m^2], the nominal frequency and wavelength for the maximum power density of blackbody radiation, f_W and λ_W, are, Fig A2-1

$$f_W = \frac{3.9207}{2.8214} = 1.39 \cdot f_{\left(W/Hz/m^2\right)}$$

$$\lambda_W = \frac{\lambda_{0\left(W/m/m^2\right)}}{3.9207} = \frac{4.9651}{3.9207} = 1.27 \cdot \lambda_{T\left(W/Hz/m^2\right)} \tag{A2:13}$$

In terms of the energy per a wavelength or a cycle of electromagnetic radiation equations (A2:8) and (A2:9) can be written in form [see equation (A1.2:2)

$$E_{\nu(W)} = \frac{F_{W(\nu,\lambda)}}{\nu} = \frac{\nu_0^2}{2c^2} \frac{(\nu/\nu_0)^2}{\left(e^{\nu/\nu_0}-1\right)} W \cdot h\nu = I_{(\nu)} \cdot h\nu = I_{(\lambda)} \cdot \frac{h_0}{\lambda} c^2 \tag{A2:14}$$

where the intensity factor $I = I_\nu = I_\lambda$ is

$$I_{(\nu)} = I_{(\lambda)} = \frac{\nu_0^2 W}{2c^2} \frac{(\nu/\nu_0)^2}{\left(e^{\nu/\nu_0}-1\right)} = \frac{W}{2\lambda_0^2} \frac{(\lambda_0/\lambda)^2}{\left(e^{\lambda_0/\lambda}-1\right)} \tag{A2:15}$$

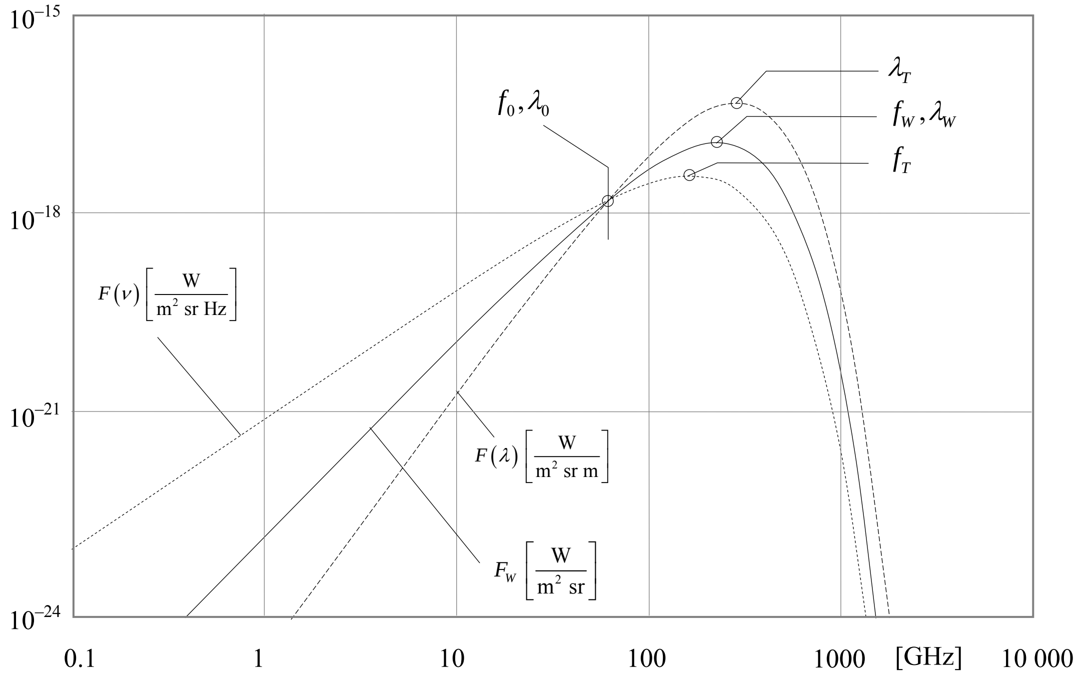

Figure B1-1. The energy flux density of black body radiation (CMB) in terms of $F(\lambda)$ [$Wm^{-2}sr^{-1}m^{-1}$] (A2:4), F_W [$Wm^{-2}sr^{-1}$] (A2:10), and $F(\nu)$ [$Wm^{-2}sr^{-1}Hz^{-1}$] (A2:5) in the frequency range from 100 MHz to 10 THz. The wavelength of the observed maximum power density in terms of $F(\nu)$ [$Wm^{-2}sr^{-1}Hz^{-1}$] is 1.87 mm. In terms of $F(\lambda)$ [$Wm^{-2}sr^{-1}m^{-1}$] the maximum occurs at wavelength 1.06 mm. The integrated total energy is equal for each flux density functions. Curve F_W [$Wm^{-2}sr^{-1}$] shows the shape of the flux density function observed in narrow band filters with $W = \Delta\lambda/\lambda = \Delta\nu/\nu$.

Equation (A2:14) shows the energy of a cycle of radiation at wavelength λ receivable with a narrowband filter with relative width $W = \Delta\lambda/\lambda = \Delta\nu/\nu$. The blackbody source is characterized by $\lambda_0 = hc/kT$. In terms of mass equivalence, and by observing the different velocities c and c_0 related to the DU concept, equation (A2:14) is written

$$E_{\nu(W)} = \frac{h_0}{\lambda} c_0 c = \frac{W h_0}{2\lambda_0^3} \frac{\left(\lambda_0/\lambda\right)^3}{\left(e^{\lambda_0/\lambda} - 1\right)} c_0 c = m_\lambda c_0 c \qquad \text{(A2:16)}$$

where the mass equivalence of wavelength λ is

$$m_\lambda = \frac{W h_0}{2\lambda_0^3} \frac{\left(\lambda_0/\lambda\right)^3}{\left(e^{\lambda_0/\lambda} - 1\right)} \qquad \text{(A2:17)}$$

*****